AD_____

Award Number: W81XWH-06-1-0120

TITLE: Evaluation of Genomic Instability in the Abnormal Prostate

PRINCIPAL INVESTIGATOR: Christina Haaland-Pullus
Jeffrey K Griffith, Ph.D.

CONTRACTING ORGANIZATION: University of New Mexico
Albuquerque, NM 87131-5221

REPORT DATE: December 2006

TYPE OF REPORT: Annual

PREPARED FOR: U.S. Army Medical Research and Materiel Command
Fort Detrick, Maryland 21702-5012

DISTRIBUTION STATEMENT: Approved for Public Release;
Distribution Unlimited

The views, opinions and/or findings contained in this report are those of the author(s) and should not be construed as an official Department of the Army position, policy or decision unless so designated by other documentation.

REPORT DOCUMENTATION PAGE

Public reporting burden for this collection of information is estimated to average 1 hour per response, including the time for reviewing instructions, searching existing data sources, gathering and maintaining the data needed, and completing and reviewing this collection of information. Send comments regarding this burden estimate or any other aspect of this collection of information, including suggestions for reducing this burden to Department of Defense, Washington Headquarters Services, Directorate for Information Operations and Reports (0704-0188), 1215 Jefferson Davis Highway, Suite 1204, Arlington, VA 22202-4302. Respondents should be aware that notwithstanding any other provision of law, no person shall be subject to any penalty for failing to comply with a collection of information if it does not display a currently valid OMB control number. **PLEASE DO NOT RETURN YOUR FORM TO THE ABOVE ADDRESS.**

1. REPORT DATE 01-12-2006	2. REPORT TYPE Annual	3. DATES COVERED 1 Dec 2005 – 30 Nov 2006
4. TITLE AND SUBTITLE Evaluation of Genomic Instability in the Abnormal Prostate		**5a. CONTRACT NUMBER**
		5b. GRANT NUMBER W81XWH-06-1-0120
		5c. PROGRAM ELEMENT NUMBER
6. AUTHOR(S) Christina Haaland-Pullus Jeffrey K Griffith, Ph.D. Email: chaaland@salud.unm.edu		**5d. PROJECT NUMBER**
		5e. TASK NUMBER
		5f. WORK UNIT NUMBER
7. PERFORMING ORGANIZATION NAME(S) AND ADDRESS(ES) University of New Mexico Albuquerque, NM 87131-5221		**8. PERFORMING ORGANIZATION REPORT NUMBER**
9. SPONSORING / MONITORING AGENCY NAME(S) AND ADDRESS(ES) U.S. Army Medical Research and Materiel Command Fort Detrick, Maryland 21702-5012		**10. SPONSOR/MONITOR'S ACRONYM(S)**
		11. SPONSOR/MONITOR'S REPORT NUMBER(S)

12. DISTRIBUTION / AVAILABILITY STATEMENT
Approved for Public Release; Distribution Unlimited

13. SUPPLEMENTARY NOTES
Original contains colored plates: ALL DTIC reproductions will be in black and white.

14. ABSTRACT

The aim of this study is to investigate the field effect in prostate cancer, the relationship between tumor and nearby histologically normal tissues compared to truly disease free prostate tissue. Identification of changes within tumor adjacent tissues has two possible clinical implications: prognosis and diagnosis. Several tools are being used to investigate this effect, specifically the assessment of telomere length, allelic imbalance, and methylation status, all markers of genomic instability. Microarray studies will be used to aid in the identification of additional gene expression changes occurring between tumor and histologically normal tissues compared to truly disease free tissue. While telomere length and allelic imbalance have been shown to correlate with outcome, it is expected that, when compared with truly normal tissue from disease-free prostates, several progressive changes will be seen, as has been found in prostate cancer cell lines. The proposed study will allow for interaction with other scientists, exposure to new technologies, teaching and continued patient interaction, all of which are important to the physician scientist.

15. SUBJECT TERMS
Prostate Cancer, Telomeres, Methylation, Micro array, Slot Blot, Allelic Imbalance

16. SECURITY CLASSIFICATION OF:			17. LIMITATION OF ABSTRACT	18. NUMBER OF PAGES	19a. NAME OF RESPONSIBLE PERSON USAMRMC
a. REPORT U	**b. ABSTRACT** U	**c. THIS PAGE** U	UU	47	**19b. TELEPHONE NUMBER** *(include area code)*

Table of Contents

I.   Introduction

The aim of this study is to investigate the field effect in prostate cancer, the relationship between tumor and nearby histologically normal tissues compared to truly disease free prostate tissue. Identification of changes within tumor adjacent tissues has two possible clinical implications: prognosis and diagnosis. Several tools are being used to investigate this effect, specifically the assessment of telomere length, allelic imbalance, and methylation status, all markers of genomic instability. Microarray studies will be used to aid in the identification of additional gene expression changes occurring between tumor and histologically normal tissues compared to truly disease free tissue. While telomere length and allelic imbalance have been shown to correlate with staging, it is expected that, when compared with truly normal tissue from disease-free prostates, several progressive changes will be seen, as has now been found in prostate cancer cell lines. The proposed study will allow for interaction with other scientists, exposure to new technologies, teaching and continued patient interaction, all of which are important to the physician scientist. While some technical difficulties have been encountered regarding assay development for aim two, they have been worked out and will not impede overall progress of the studies proposed.

Hypothesis and Rationale
It is currently thought that a multi-step process is involved in the development of prostate cancer. Preliminary data from our laboratory suggests that telomere content (TC) and allelic imbalance (AI) is altered in both tumor and tumor adjacent tissue, and that these changes precede histologic changes. It is reasonable to extrapolate from this that normal appearing tissue may have diagnostic properties. Our data also suggests that there is a relationship between the level of genomic instability and relapse regarding prostate cancer, indicating that this tissue may also have prognostic significance. While TC is a useful marker, the slot blot assay, developed within our laboratory, is time intensive, difficult, and requires a large amount of starting material. Polymerase chain reaction (PCR) based assays may prove to be as informative and more easily translatable to the clinical setting, as this may be able to utilize the limited supply of cells obtained during a biopsy. AI is one possible technique that appears to be predictive within the laboratory, and preliminary results indicate that an assay for promoter methylation may also be useful. Because the TC and AI modalities have previously shown correlation between staging and outcome, these will be used to determine the effectiveness of the methylation assay. Additionally, this study will use microarray analysis to help guide the determination of where to look for changes in methylation status based on expression changes, as this will allow determination of expression differences between tumor, tumor adjacent tissues, and disease free prostate tissues.

Specific Aim #1: *Further assess and refine the use of the allelic imbalance assay in predicting potential disease relapse in retrospective and prospective studies of prostate cancer.*

Specific Aim #2: *Compare methylation states of genes known to be associated with prostate cancer, such as GSTP1, P504S, and CD44, between tumor cells, PHN tissue and normal prostate tissue from men without cancer.*

Specific Aim #3: *Assess characteristic changes in gene expression with microarray relevant to prognosis in prostate cancer, and determine if this profile extends to surrounding histologically normal cells.*

II.   Key Research Accomplishments

IIa.   Research Accomplishments

- Developed an assay for detecting methylation at specific gene promoters

- Methylation of prostate cancer cell line models has been characterized for specific promoters. (Appendix A, figure 1, 4).

- Methylation of normal prostate and buchal DNA has been characterized. (Appendix A, figure 2).

- Preliminary characterization of gene promoter methylation of prostate tumor and tumor adjacent tissue in a collection of matched samples for a set of genes. (Appendix A, figure 3, 4).

- Methylation within the set of cases currently characterized shows changes between tumor and tumor adjacent tissues. (Appendix A, figure 3).

- Co-authored a paper regarding field effect in breast tissue. (Appendix B).

- Co-authored a paper demonstrating the use of allelic imbalance as a measurement of genomic instability. (Appendix C).

IIb.   <u>Training and Educational Accomplishments</u>

The PhD candidate has had continuing opportunities to work and interact with oncologists, pathologists and other PhD scientists who specialize in prostate cancer. These interactions have occurred through tumor board meetings, journal clubs, urology rounds, special seminars and direct interaction within the clinical setting as well as the laboratory. Training in microscopy has taught the candidate recognition of the various pathologies of the prostate. Additionally, she has been active in patient enrollment for prognostic studies and has learned how to design a study, and the administrative requirements associated with clinical research. This type of interaction is also valuable, as it provides ongoing interaction with patients, something the candidate feels is important to her career as a physician scientist.

On an educational level, the candidate has completed all required course work for completion of a PhD degree. The candidate has also assisted in the writing and the co-instruction of a section of the upper-level undergraduate course, Biochemical Laboratory Methods. The candidate has aspirations of continuing her career in research and remaining in academia and felt teaching provided an opportunity to develop the essential teaching skills need for her chosen career path as a physician scientist.

IIc.   Performance Accomplishments

Experimental Milestones
Specific Aim One: (7 tasks) To refine the use of allelic imbalance (AI) and telomere content (TC) in staging disease progression in the prostate through retrospective and prospective studies.

Tasks 1:   Months 1-6   **Ongoing**
-Identify and acquire archival specimens from the New Mexico Tumor Registry (NMTR) and the University of New Mexico School of Medicine (UNMSOM) based on recurrence/remission status for retrospective study.

Samples have been identified and collected. TC and AI have been analyzed for retrospective cases. Identification and collection of additional prospective cases is ongoing.

Task 2:   Months 6-8   **Completed**
-Isolate DNA from archival samples.

DNA has been isolated for retrospective cases.

Task 3:   Months 1-8   **Completed**
-Identify additional AI probes to assess for prostate cancer specificity.

Additional probes have been identified based on a review of the current literature.

Task 4:   Months 8-10   **Ongoing**
-Measure AI.

AI has been measured for the archival tissues. AI assessment of prospective tissues is ongong.

Task 5:   Months 10-12   **Ongoing**
-Analyze data

Analysis of the data will occur as appropriate DNA for this arm of the study becomes available.

Task 6:   Months 1-28   **Ongoing with modification**
-Acquire samples from UNMSOM on an ongoing basis for prospective study. Isolate and assess DNA using AI and TC assays.

The student has been enrolling patients into a prospective study to assess telomeres and diagnosis. The samples have been acquired at the Veteran's Affairs Hospital (VAH). Samples are currently being acquired and stored for use analysis by TC and AI.

Task 7:   Months 2-36   **Ongoing**
        -Compare prospective study data with pathology reports and outcome to correlate AI and TC results with diagnosis and disease progression.

        Data is being collected on an ongoing basis for this task.

Specific Aim Two: (8 tasks) Evaluate methylation of prostate-specific genes and field effect.

Task 1:   Months 1-6   **Completed with modification**
        -Identify and acquire specimens from NMTR and UNMSOM based on recurrence/remission status.

        Samples have been identified based on matched tissue status and previous analysis by TC and AI. Twelve cases were chosen, in accordance with the proposed 10-15 cases.

Task 2:   Months 6-8   **Completed**
        -Isolate and prepare DNA from samples.

        DNA has been isolated from the twelve matched cases.

Task 3:   Months 8-12   **Ongoing**
        -Assess the methylation status of specific genes.

        The student has identified several genes of interest fro ma thorough review of the current literature. The student has worked out the methods of detecting a genes status as methylated or unmethylated, although this took longer than expected. Gene methylation status detection of patient samples and prostate cancer cell line models is currently ongoing.

Task 4:   Months 12-14   **Ongoing**
        -Analyze data generated.

        Data is being analyzed on an ongoing basis.

Task 5:   Months 14-18   **Not initiated**
        -Identify and obtain additional samples, including those from aim one.

        The student is on schedule for this task.

Task 6:   Months 18-22   **Not initiated**
        -Isolate and prepare DNA.

        The student is on schedule for this task.

Task 7:   Months 22-26   **Not initiated**
          -Assess methylation of original and additional genes found in aim two.

          The student is on schedule for this task.

Task 8:   Months 26-30   **Not initiated**
          -Final analysis of data.

          The student is on schedule for this task.

Specific Aim Three: (8 tasks) Use microarray gene expression analysis to identify gene expression profiles, changes occurring with respect to field effect, and identify additional genes associated with prostate cancer.

Task 1:   Months 1-6   **Completed**
          -Identify and acquire archival specimens from NMTR and UNMSOM based on recurrence/remission status for retrospective study.

          Specimens previously analyzed by TC and AI and with matched tumor and 1 cm nearby tissue from 12 patients were identified for this specific aim.

Task 2:   Months 6-10   **Completed**
          -Isolate RNA from archival samples, convert to cDNA for microarray assay.

          The student isolated RNA from the 12 matched cases of tumor and 1 cm nearby tissue.

Task 3:   Months 10-14   **In progress**
          -Run microarray analyses.

          The student is scheduled to perform the analysis as the facility's prior commitments allow.

Task 4:   Months 14-18   **Not initiated**
          -Analyze data, identifying additional genes for investigation by AI, TC or methylation assays. Compile preliminary genetic profiles.

          This will commence upon completion of the micro array analysis of the 12 matched samples noted above.

Task 5:   Months 18-20   **Not initiated**
          -Identify and acquire additional specimens from the prospective study in aim one, NMTR, and UNMSOM based on recurrence/remission status.

          The student is on schedule to begin this task.

Task 6:   Months 20-24   **Not initiated**
          -Isolate RNA from samples, convert to cDNA for microarray assay.

          The student is on schedule to begin this task.

Task 7:   Months 24-28   **Not initiated**
          -Run microarray analyses.

          The student is on schedule to begin this task

Task 8:   Months 28-30   **Not initiated**
          -Final analysis of data with evaluation of predictive value.

          The student is on schedule to begin this task

Aims One, Two, and Three:
Months 10-36: Prepare and submit manuscripts.

Educational and Training Milestones (3 tasks)
Task 1:   Months 1-12   **Completed with modification**
          -Develop ability to identify the morphology and characteristics of prostate tissue from
          normal to metastatic cancer. Learn the use of special stains and histological markers in
          prostate pathology. This will be done under the instruction of Dr. Nancy Joste, Chief of
          Surgical Pathology.

          The student has learned identification of various stages of prostate cancer, as well as the
          normal pathology of the prostate gland. The training was carried out at the Veteran's
          Affairs Hospital (VAH) in Albuquerque in the pathology department with Dr. Massie.
          This change occurred as the VAH has more prostate cases and the student has been
          enrolling patients here and Dr. Massie, the head of the Pathology Department, has been
          providing pathologic information regarding study subjects.

Task 2:   Months 1-36   **Continuing with modification**
          -Attend clinics with oncologists (Dr. Ian Rabinowitz, Dr. Anthony Smith) at the
          University of New Mexico Hospital for the purpose of directly observing current
          detection, diagnosis, and treatment of prostate cancer, and to learn about the patient's
          interactions, perceptions and concerns with these current modalities. Attend oncology
          rounds and meetings at the Cancer Research and Treatment Center to expand general and
          detailed knowledge base of oncology.

          The student has been observing surgeries at the VAH with Dr. Michael Davis. This
          change was made due to the higher frequency of prostatectomies at the VAH. The student

has been attending urology rounds as well as directly interacting with prostate cancer patients.

Task 3:   Months 12-36   **Not initiated**
-Present ongoing work at local and national meetings.

The student will begin this task as presentable results are acquired during the remaining years as appropriate. However, the student did attend the annual MD/PhD conference in July 2006 in Keystone, Colorado, an event the student feels is beneficial due to the interaction opportunities it allows her with other physician scientist students from across the country.

III.   Reportable Outcomes

Journal Articles

C.M. Heaphy, M.Bisoffi, C.A. Fordyce, **C.M. Haaland**, W.C. Hines, N.E. Joste and J.K. Griffith. Telomere DNA content and allelic imbalance demonstrate field cancerization in histologically normal tissue adjacent to breast tumors. International Journal of Cancer, 119:108-116, 2006. (Appendix B).

C.M. Heaphy, W.C. Hines, K.S. Butler, **C.M. Haaland**, G. Heywood, E.G. Fischer, M. Bisoffi and J.K. Griffith. Measurement of Genome-wide Allelic Imbalance in Human Tissue Using a Multiplex PCR System. Journal of Molecular Diagnotics (in press). (Appendix C).

IV.   Conclusions

TC and AI studies are ongoing regarding the prospective arm of specific aim one, and completed for the retrospective aspect of the same aim. While set backs regarding the methylation assay development have occurred, the student is still on schedule to reach the goals of the proposal. The student has developed the assay required to determine gene promoter methylation status, and has used this assay to characterize prostate cancer model cell lines, as well as completing preliminary work in patient samples. Microarray studies are on schedule, with samples identified and prepared for analysis. The student has co-authored two papers, one regarding the field effect within breast tissue, and the other regarding the use of allelic imbalance as a means of assessing genomic stability in tumor and tumor adjacent tissues. While the first paper is regarding the breast environment, the student felt that this was still worth while to work on as it is still an androgen dependant malignancy, as prostate tumors are. Additionally, the work done allowed the student to master the slot blot assay for measuring TC. The second paper, regarding allelic imbalance, allowed the student to master the technique of measuring AI. Education milestones are on currently on track, with the student ready to begin presenting data at national meeting such s the Department of Defense IMPaCT meeting in September, 2007, as well as the annual MD/PhD conference in Keystone, Colorado in 2007.
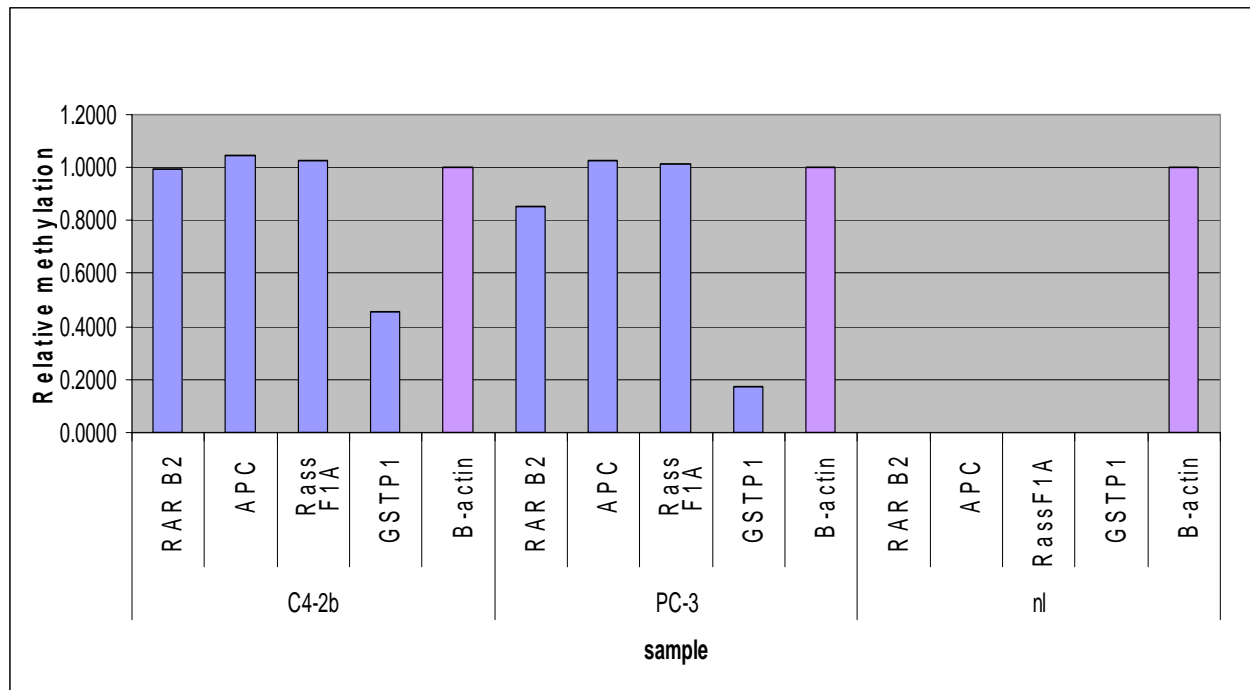
Appendix A

Figure 1

Figure 1. The methylation status of two prostate cancer cell line models, C4-2b, a bone metastasis, androgen independent model, and PC-3, an androgen independent model, have been characterized for the genes Rar-B2, APC, Rass F1A, and GSTP-1. Included in the graph is normal buchal DNA for reference. C4-2b and PC-3 are methylated at the promoters to varying degrees for all four genes, while normal buchal DNA shows no methylation at any of these sites. B-actin detection is for the unmethylated gene promoter, and is used as an internal reference to normalize the assay.

Figure 2
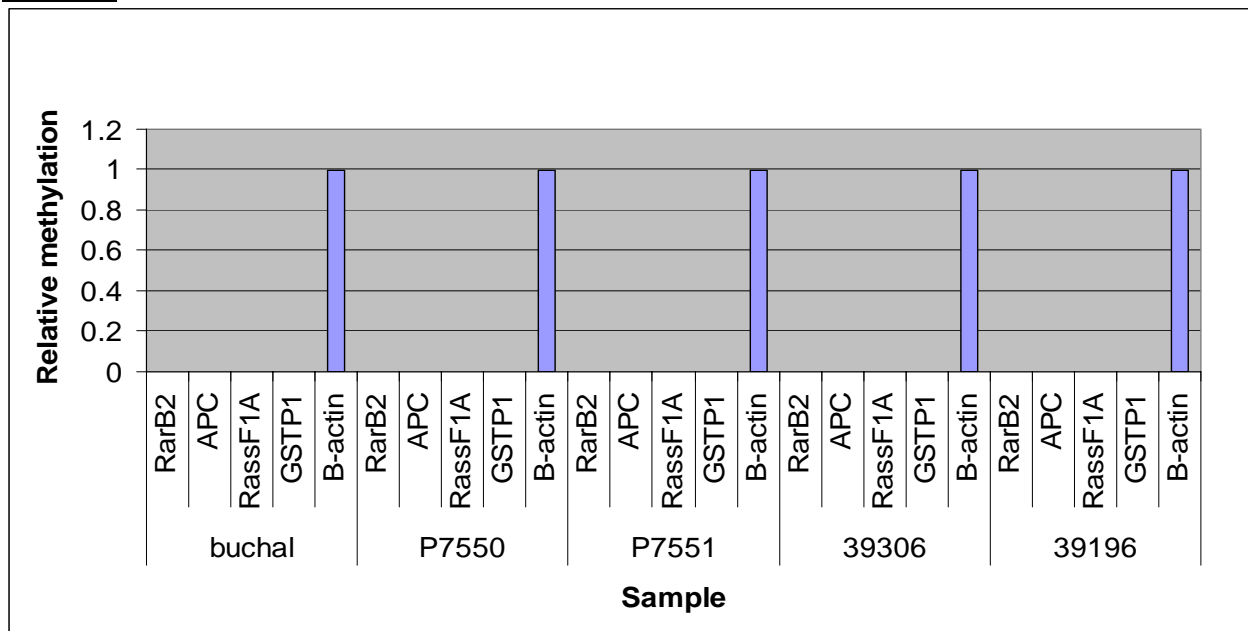
Figure 2. DNA from non-cancerous tissues. Included are buchal DNA, two post-mortem DNA samples of prostate tissue from infants (P7550, P7551), and two post-mortem DNA samples from adults shown to be free of prostate disease (39306, 39196). All samples were analyzed for methylation with the promoters for Rar-B2, APC, Rass F1A, and GSTP-1. In all cases all gene promoters were found to be unmethylated. Unmethylated B-actin is the internal reference control used to normalize assay results.

Figure 3
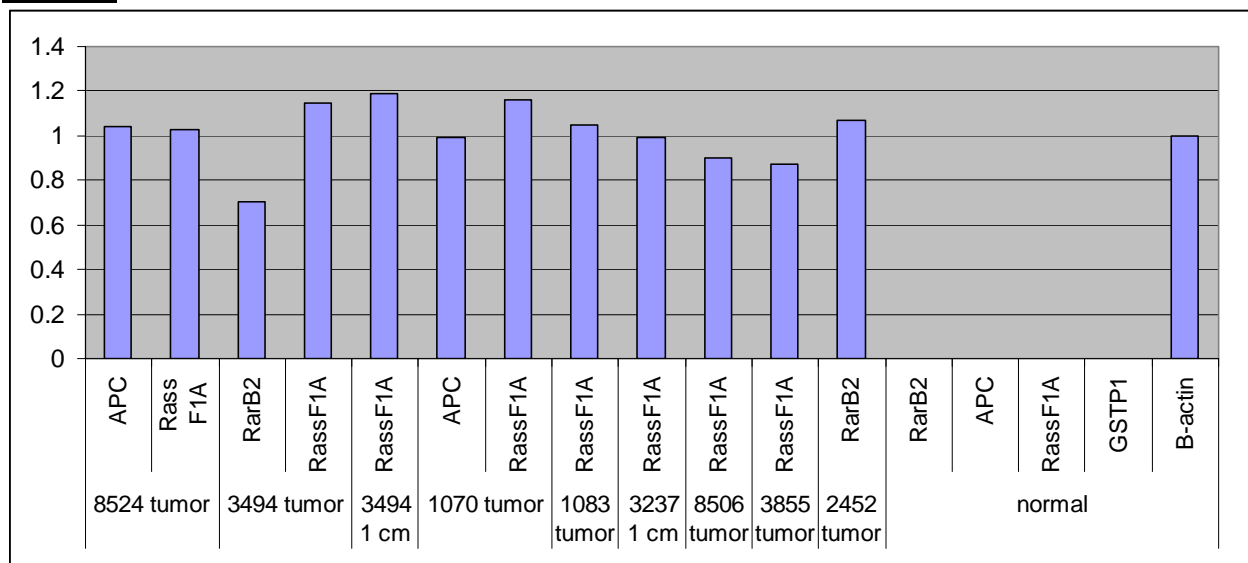
Figure 3. Methylation results for eight cases of tumor and matched 1 cm tissue. Only methylated genes are included in the graph. Each matched set was evaluated for APC, RassF1A, RarB2,

15

GSTP1, and B-actin as the non-methylated control reference. The results of normal buchal DNA are included for reference purposes, and unmethylated B-actin is the internal reference, shown for comparison purposes. A value of 1 or greater indicates full methylation and gene silencing in all cases except B-actin, where 1 indicates a non-methylated promoter. Patient designation and sample source are indicated at the bottom; the scale at left represents relative methylation.
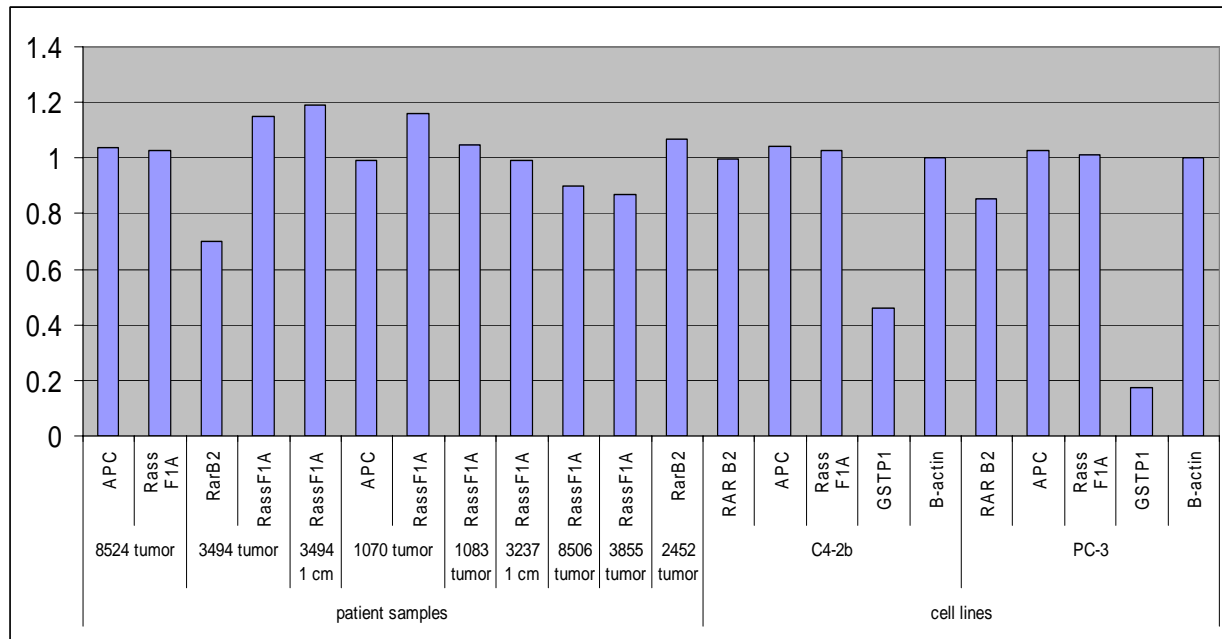
Figure 4

Figure 4. Relative gene promoter methylation levels are shown for patient cases compared to cell line models. This graph demonstrated the variable nature of individual patient samples in comparison to that of progressively aggressive cell line models.

Appendix B

Assessment of Genome-wide Allelic Imbalance in Human Tissue Using a Multiplex PCR System

Christopher M. Heaphy[1], William C. Hines[1,5], Kimberly S. Butler[1], Christina M. Haaland[1], Glenroy Heywood[2,4], Edgar G. Fischer[3], Marco Bisoffi[1,4] and Jeffrey K. Griffith[1,4]

Departments of [1]Biochemistry and Molecular Biology, [2]Surgery, [3]Pathology, and the [4]Cancer Research and Treatment Center, University of New Mexico School of Medicine, Albuquerque, New Mexico.

[5]Current Address: Division of Life Sciences, Lawrence Berkeley National Laboratory, Berkeley, California.

# of text pages: 17; # of tables: 0; # of figures: 3

Running Title: Assessment of Genome-wide AI in Human Tissues

Request for reprints: Jeffrey K. Griffith, Ph.D., Department of Biochemistry and Molecular Biology, MSC08 4670, 1 University of New Mexico, Albuquerque, New Mexico 87131-0001. Phone: 505-272-3444; Fax: 505-272-6587; Email: jkgriffith@salud.unm.edu

Abstract

Genomic instability can generate chromosome breakage and fusion randomly throughout the genome, frequently resulting in allelic imbalance, which is a deviation from the normal 1:1 ratio of maternal and paternal alleles. Thus, it is reasonable to speculate that tissues with more sites of allelic imbalance have a greater likelihood of having disruption of any of the numerous critical genes that cause a cancerous phenotype, and thus may have diagnostic or prognostic significance. For this reason, it is desirable to develop a robust method to provide a global assessment of genomic instability in any tissue. To address this need, we designed an economical and high-throughput method, based on the Applied Biosystems AmpFℓSTR® Identifiler multiplex PCR system, to evaluate allelic imbalance at 16 unlinked, microsatellite loci located throughout the genome. This method provides a quantitative comparison of the extent of allelic imbalance between samples that can be applied to a variety of frozen and archival tissues. The method does not require matched normal tissue, requires very little DNA (the equivalent of approximately 150 cells) and uses commercially available reagents, instrumentation and analysis software. Greater than 99% of tissue specimens with ≥ 2 unbalanced loci were cancerous.

Introduction

It is widely accepted that genomic instability- the duplication, loss or structural rearrangement of a critical gene(s) - occurs in virtually all cancers[1], and in some instances has diagnostic, prognostic or predictive significance. Thus, it is not surprising that tumor progression is reflected by allelic losses or gains in genes that regulate aspects of cell proliferation, apoptosis, angiogenesis, invasion and, ultimately, metastasis.[2,3]

There are several technologies available to detect allelic imbalance (AI), which is a deviation from the normal 1:1 ratio of maternal and paternal alleles. For example, chromosome painting techniques can identify AI in cytological preparations.[4,5] However, these methods are poorly suited for high-throughput applications and analysis is limited to a relatively small cellular field, thus increasing potential sampling error. Single nucleotide polymorphism (SNP) arrays can be used for high-resolution genome-wide genotyping and loss of heterozygousity (LOH) detection.[6-8] For example, the development of a panel of 52 microsatellite markers that detects genomic patterns of LOH [9-11] has been utilized for breast cancer diagnosis and prognosis. However, this approach requires matched referent (normal) DNA and these organ-specific panels may not be informative for other cancer types, thus limiting their applicability across multiple tumor types.

Larger panels of SNPs may be used for genome-wide analysis, for example the Affymetrix 10K and 100K SNP mapping arrays.[12-13] Likewise, Illumina BeadArrays with a SNP linkage-mapping panel,[14] allow allelic discrimination directly on short genomic

3

segments surrounding the SNPs of interest, thus overcoming the need for high-quality

DNA.[8] Lips and colleagues have shown that Illumina BeadArrays can be used to obtain

reliable genotyping and genome-wide LOH profiles from formalin-fixed, paraffin-

embedded (FFPE) normal and tumor tissues.[15] Another method of detecting segmental

genomic alterations is comparative genomic hybridization (CGH). CGH identifies copy-

number changes by detecting DNA sequence copy variations throughout the entire

genome and mapping them onto a cytogenetic map supplied by metaphase

chromosomes.[16] Alternatively, array CGH maps copy number aberrations relative to the

genome sequence by using arrays of BAC or cDNA clones as the hybridization target

instead of the metaphase chromosomes.[17-21] However, all these approaches, while robust,

require costly reagents, specialized equipment, and the sheer amount of data produced

from these analyses complicate the interpretation of results.

For these reasons, and as outlined by Davies et al.,[22] it is desirable to develop a general,

economical, and high-throughput method to provide a global assessment of genomic

instability in any tissue, independent of the nature and composition of the specimen and

the availability of matched, normal tissue. To address this need, we developed a method

to measure the ratio of maternal and paternal alleles at 16 unlinked, microsatellite short

tandem repeat (STR) loci in a single multiplexed PCR reaction. The assay, which is based

on the Applied Biosystems AmpFℓSTR® Identifiler system, can be performed with only

1 ng of genomic DNA, uses commercially available primers and reagents, and common

instrumentation and analysis software. Thus, it is an attractive alternative to current

methods that is readily adaptable to most clinical laboratory environments.

Materials and Methods

Tissue Acquisition: All tissues were provided by the University of New Mexico Solid Tumor Facility, unless otherwise specified. Buccal cells were collected from oral rinses of volunteers. The Cooperative Human Tissue Network (Western Division, Nashville, TN) provided frozen normal and tumor renal tissues, obtained by radical nephrectomy, frozen normal breast tissues, obtained by reduction mammoplasty, and normal frozen prostate tissues, obtained through autopsy. A set of FFPE prostate tumors, obtained by radical prostatectomy, were provided by the Cooperative Prostate Cancer Tissue Resource (http://www.cpctr.cancer.gov). Duodenal FFPE tumor tissues were obtained from the Mayo Clinic (Rochester, MN). Pancreatic FFPE normal and tumor tissues were obtained from the Department of Pathology at the University of New Mexico. Frozen endometrial tumor tissues were obtained through the Gynecologic Oncology Group (Philadelphia, PA). All specimens lacked patient identifiers and were obtained in accordance with all federal guidelines, as approved by the UNM Human Research Review Committee.

DNA Isolation and Quantification: DNA was isolated from all tissue samples using the DNeasy® silica-based spin column extraction kit (Qiagen; Valencia, CA) and the manufacturer's suggested animal tissue protocol. FFPE samples were treated with xylene and washed with ethanol prior to DNA extraction. DNA concentrations were measured using the Picogreen® dsDNA quantitation assay (Molecular Probes, Eugene, OR) using a λ phage DNA as the standard as directed by the manufacturer's protocol.

Multiplex PCR Amplification of STR Loci: The AmpFℓSTR® Identifiler kit (Applied Biosystems, Foster City, CA) was used to amplify genomic DNA at 16 different short tandem repeat (STR) microsatellite loci (Amelogenin, CSF1PO, D2S1338, D3S1358, D5S818, D7S820, D8S1179, D13S317, D16S539, D18S51, D19S433, D21S11, FGA, TH01, TPOX and vWA) in a single multiplexed PCR reaction, according to the supplier's protocol. Linear amplification of allelic PCR products is a prerequisite for ratiometric determination of AI. Therefore, each PCR reaction was limited to 28 cycles, as determined in preliminary studies. The 16 primer sets are designed and labeled with either 6-FAM, PET, VIC or NED to permit the discrimination of all amplicons in a single electrophoretic separation. The PCR products were resolved by capillary electrophoresis using an ABI Prism® 377 DNA Sequencer (Applied Biosystems, Foster City, CA). Fluorescent peak heights were quantified using ABI Prism GeneScan® Analysis software (Applied Biosystems, Foster City, CA). Allelic ratios were calculated using the peak height, rather than the peak area, as suggested in previous studies.[23-25] For simplicity, the allele with the greater fluorescence was always made the numerator, as to always generate a ratio ≥ 1.0.

Statistical Analysis: A Pearson Chi-square test was performed using SAS JMP® software version 9.1 (SAS Institute Inc., Cary, NC) to examine the relationship between the extent of AI and tissue type, using a significance level of 0.05.

Results

The 16 allelic microsatellite loci amplified by the AmpFℓSTR® Identifiler primer sets are unlinked, and can be used to assess AI simultaneously at multiple heterozygous sites throughout the genome. This is technically possible because each amplicon is labeled with one of four fluorescent dyes (6-FAM, PET, VIC and NED), each with a unique emission profile, thus allowing the resolution of amplicons of similar size. Figure 1 shows the sizes of VIC-labeled amplicons derived from a representative specimen of matched normal and tumor renal tissue (the fluorescent channels showing the PET, 6-FAM, and NED-labeled products are not shown). Within Figure 1A, illustrating the results from the normal tissue specimen, two of the allelic pairs are homozygous (D13S317, D16S539), as indicated by a single peak, and three of the allelic pairs are heterozygous (D3S1358, TH01, D2S1338), as indicated by two peaks. Although the peak heights varied between different loci, ostensibly due to different PCR efficiencies, the peak heights of the paired alleles were similar. Theoretically, the ratio of any two heterozygous alleles following PCR amplification would be 1.0 in normal tissues. To test this premise, the ratios of paired alleles' signal intensities were compared at 320 heterozygous loci in buccal cells from 27 healthy individuals. As expected, the mean ratio was near 1.0 (mean =1.15, SD 0.18). We expect that approximately 97.5% of all allelic ratios in normal tissues would fall within 2.5 SD of the mean, and therefore operationally defined an allelic ratio of >1.60 (mean + 2.5 SD) as a site of AI. Applying this threshold to the 27 analyzed buccal samples, only 8 sites of AI were detected out of the 320 heterozygous loci, thus representing a mean of 0.30 unbalanced loci per sample. Figure 1B illustrates the results of the tumor tissue matched to the normal sample in

Figure 1A. Within this sample, two of the three heterozygous loci in the renal tumor tissue amplified by the VIC-labeled primer sets have peak height ratios of >1.60, identifying them as sites of AI.

To determine whether AI determinations were reproducible, the assay was repeated within a random subset of the buccal samples. Figure 2A shows that 193 of the 198 (97.5%) loci measured were correctly categorized upon repeating the experiment; whereas, only 5 of the 198 (2.5%) loci initially designated as sites of AI could not be confirmed. Two loci changed from sites without AI (≤ 1.60) to sites of AI (> 1.60) and three loci changed from sites of AI to sites without AI.

We next confirmed that the differences in AI detected by this approach reflected true differences in the ratio of the alleles, and not experimental artifact (e.g. differential PCR amplification efficiency), we constructed defined mixtures of DNAs from the paired normal and tumor tissue shown in Figure 1. As shown in Figure 2B for the D3S1358 locus, there was a linear relationship (R^2=0.965) between the ratio of alleles measured in the assay and the composition of the mixture. Similar results were obtained for each of the other loci exhibiting a site of AI (TH01: R^2=0.973; VWA: R^2=0.981; D18S541: R^2=0.953). In contrast, the composition of the mixture had no effect on the allelic ratios of loci not exhibiting AI (data not shown).

The operationally-defined threshold for AI was validated by measuring the allelic ratios for 1382 heterozygous loci in an independent test set comprised of 118 normal samples

consisting of bone (n=2), breast (n=10), buccal (n=53), lymph node (n=5), peripheral

blood lymphocytes (PBL) (n=18), pancreas (n=6), placenta (n=3), prostate (n=4), renal

(n=16) and tonsil (n=1) tissues (Figure 3A). In this sample set of normal tissues, only 32

of 1382 heterozygous loci were designated sites of AI, thus representing a mean of 0.27

unbalanced loci per sample, comparable to the 0.30 unbalanced loci per sample in the

original normal sample set. In summary, 88 (74.6%), 29 (24.6%), and 1 (0.8%) of the 118

normal tissues specimens contained 0, 1 and 2 loci with AI, respectively.

We hypothesized that AI was associated with gene disruption and aberrant expression,

implying that cancerous tissues would have more sites of AI than normal tissues. To test

this hypothesis, we next measured the frequency of AI in 2792 heterozygous loci in a set

of 239 frozen or FFPE tumor samples consisting of AML (n=8), breast (n=39), CML

(n=3), duodenal (n=23), endometrial (n=78), pancreas (n=6), prostate (n=47), and renal

(n=35) tissues. As shown in Figure 3B, 37 (15.5%), 41 (17.2%), and 161 (67.4%) of the

239 tumor tissues specimens contained 0, 1 and $\geq$ 2 loci with AI, respectively. In

contrast to the normal tissues, 611 sites of AI were detected, thus representing a mean of

2.56 unbalanced loci per sample, nearly 10 times greater than the frequency in the normal

tissues (p < 0.0001). In summary, 162 of 357 tissue specimens had $\geq$ 2 unbalanced loci,

of which >99% were cancerous.

Discussion

Manifestations of genomic instability, such as AI, are widespread in solid tumors.[1] There

have been numerous studies of these abnormalities and several techniques, including

chromosome painting, array CGH and SNP arrays, have emerged to analyze these differences between normal and tumor tissues.[4-21] However, these methods are typically costly, time intensive, and need a matched referent (normal) DNA sample for analysis. For this reason, it is desirable to develop general, economical, high-throughput methods to quantify the extent of AI in the genome of any tissue, independent of the nature and composition of the specimen and the availability of matched, normal tissue.

Using our newly developed assay and interpretation scheme to assess the extent of genome-wide unlinked AI in human tissues, we have shown in a set of 239 samples that 67% of the tumors contained two or more sites of AI, as compared to 0.8% of the normal samples, which represents an almost 84 fold difference. It must also be noted that this method provides a minimum estimate of AI, since the assay cannot discriminate between homozygous alleles and complete loss of heterozygosity in the absence of matched normal tissue. However, this limitation is mitigated by the near ubiquitous presence of normal tissue within tumors which allows for the assessment of AI in samples without requiring analysis of matched normal tissue. This is an important consideration in the potential evaluation of biopsy tissue, which may contain multiple clones of genetically altered cells superimposed on a background of normal stromal and epithelial cells and obtaining matched normal tissue may be difficult.

Altered gene expression resulting from genomic instability is a cause of cancer progression. We therefore hypothesized that cancerous tissues would have more sites of AI than normal tissues. Consistent with this hypothesis, >99% of tissues with ≥2 sites of

AI were cancerous. Therefore, we are currently investigating the possibility that the *number* of sites of AI in cancer tissue is a reflection of its stage of progression, and therefore may be correlated with clinical parameters or prognosis.

In conclusion, we describe here a simple method for assessing the extent of AI throughout the genome. This method has a number of significant advantages over existing technologies, such as chromosome painting, array CGH and SNP arrays, and as a molecular based assay may be utilized clinically in conjunction with histological techniques. The advantages of this method are that: (i) it is robust, reproducible and provides a quantitative basis for comparing the extent of AI between samples; (ii) it does not require matched normal tissue; (iii) it utilizes commercially available reagents, instrumentation and analysis software; (iv) it can be applied to a variety of fresh, frozen and archival tissues; (v) it requires very little DNA (the equivalent of approximately 150 cells); and (vi) >99% of tissues with ≥2 sites of AI were cancerous.

References

1. Lengauer C, Kinzler KW, Vogelstein B: Genetic instabilities in human cancers. Nature 1998, 396:643-649

2. Payne SR, Kemp CJ: Tumor suppressor genetics. Carcinogenesis 2005, 6:2031-2045

3. Hanahan D, Weinberg RA: The hallmarks of cancer. Cell 2000, 100:57-70

4. Mundle SD, Sokolova I: Clinical implications of advanced molecular cytogenetics in cancer. Expert Rev Mol Diagn 2000, 4:71-81

5. Gray JW, Collins C: Genome changes and gene expression in human solid tumors. Carcinogenesis 2000, 21:443-452

6. Rauch A, Ruschendorf F, Huang J, Trautmann U, Becker C, Thiel C, Jones KW, Reis A, Nurnberg P: Molecular karyotyping using an SNP array for genomewide genotyping. J Med Genet 2004, 41:916–922

7. Zhao X, Li C, Paez JG, Chin K, Janne PA, Chen TH, Girard L, Minna J, Christiani D, Leo C, Gray JW, Sellers WR, Meyerson M: An integrated view of copy number and allelic alterations in the cancer genome using single nucleotide polymorphism arrays. Cancer Res 2004, 64:3060–3071

8. Fan JB, Oliphant A, Shen R, Kermani BG, Garcia F, Gunderson KL, Hansen M, Steemers F, Butler SL, Deloukas P, Galver L, Hunt S, McBride C, Bibikova M, Rubano T, Chen J, Wickham E, Doucet D, Chang W, Campbell D, Zhang B, Kruglyak S, Bentley D, Haas J, Rigault P, Zhou L, Stuelpnagel J, Chee MS: Highly parallel SNP genotyping. Cold Spring Harb Symp Quant Biol 2003, 68:69-78

9. Ellsworth RE, Ellsworth DL, Lubert SM, Hooke J, Somiari RI, Shriver CD: High-throughput loss of heterozygosity mapping in 26 commonly deleted regions in breast cancer. Cancer Epidemiol Biomarkers Prev 2003, 129:915-919

10. Ellsworth DL, Ellsworth RE, Love B, Deyarmin B, Lubert SM, Mittal V, Hooke JA, Shriver CD: Outer breast quadrants demonstrate increased levels of genomic instability. Ann Surg Oncol 2004, 11:861-868

11. Ellsworth RE, Ellsworth DL, Deyarmin B, Hoffman LR, Love B, Hooke JA, Shriver CD: Timing of critical genetic changes in human breast disease. Ann Surg Oncol 2005, 12:1054-1060

12. Zhou X, Mok SC, Chen Z, Li Y, Wong DT: Concurrent analysis of loss of heterozygosity (LOH) and copy number abnormality (CNA) for oral premalignancy progression using the Affymetrix 10K SNP mapping array. Hum Genet 2004, 115:327-330

13. Meaburn E, Butcher LM, Schalkwyk LC, Plomin R: Genotyping pooled DNA using 100K SNP microarrays: a step towards genomewide association scans. Nucleic Acids Res 2006 (in press)

14. Murray SS, Oliphant A, Shen R, McBride C, Steeke RJ, Shannon SG, Rubano T, Kermani BG, Fan JB, Chee MS, Hansen MS: A highly informative SNP linkage panel for human genetic studies. Nat Methods 2004, 1:113–117

15. Lips EH, Dierssen JW, van Eijk R, Oosting J, Eilers PH, Tollenaar RA, de Graaf EJ, van't Slot R, Wijmenga C, Morreau H, van Wezel T: Reliable high-throughput genotyping and loss-of-heterozygosity detection in formalin-fixed, paraffin-

embedded tumors using single nucleotide polymorphism arrays. Cancer Res 2005, 65:10188-10191

16. Kallioniemi A, Kallionemi OP, Sudar D, Rutovitz D, Gray JW, Waldman F, Pinkel D: Comparative genomic hybridization for molecular cytogenic analysis of solid tumors. Science 1992, 258:818-821

17. Solinas-Toldo S, Lampel S, Stilgenbauer S, Nickolenko J, Benner A, Dohner H, Cremer T, Lichter P: Matrix-based comparative genomic hybridization: biochips to screen for genomic imbalances. Genes Chromosomes Cancer 1997, 20:399-407

18. Pinkel D, Segraves R, Sudar D, Clark S, Poole I, Kowbel D, Collins C, Kuo W.L., Chen C, Zhai Y, Dairkee SH, Ljung B.M., Gray JW, Albertson DG: Quantitative high resolution analysis of DNA copy number variation in breast cancer using comparative genomic hybridization to DNA microarrays. Nat Genet 1998, 20:207-211

19. Pollack JR, Perou CM, Alizadeh AA, Eisen MB, Pergamenschikov A, Williams CF, Jeffrey SS, Botstein D, Brown PO: Genome-wide analysis of DNA copy-number changes using cDNA microarrays. Nat Genet 1999, 23:41-46

20. Snijders AM, Nowak N, Segraves R, Blackwood S, Brown N, Conroy J, Hamilton G, Hindle AK, Huey B, Kimura K, Law S, Myambo K, Palmer J, Ylstra B, Yue JP, Gray JW, Jain AN, Pinkel D, Albertson DG: Assembly of microarrays for genome-wide measurement of DNA copy number. Nat Genet 2001, 29:263-264

21. Albertson DG: Profiling breast cancer by array CGH. Breast Cancer Res Treat 2003, 78:289-298

22. Davies JJ, Wilson IM, Lam WL: Array CGH technologies and their applications to cancer genomes. Chromosome Res 2005, 13:237-248

23. Paulson TG, Galipeau PC, Reid BJ: Loss of heterozygosity analysis using whole genome amplification, cell sorting, and fluorescence-based PCR. Genome Res 1999, 9:482-491

24. Medintz IL, Lee CC, Wong WW, Pirkola K, Sidransky D, Mathies RA: Loss of heterozygosity assay for molecular detection of cancer using energy-transfer primers and capillary array electrophoresis. Genome Res 2000, 10:1211-1218

25. Skotheim RI, Diep CB, Kraggerud SM, Jakobsen KS, Lothe RA. Evaluation of loss of heterozygosity/allelic imbalance scoring in tumor DNA. Cancer Genet Cytogenet 2001, 127:64-70
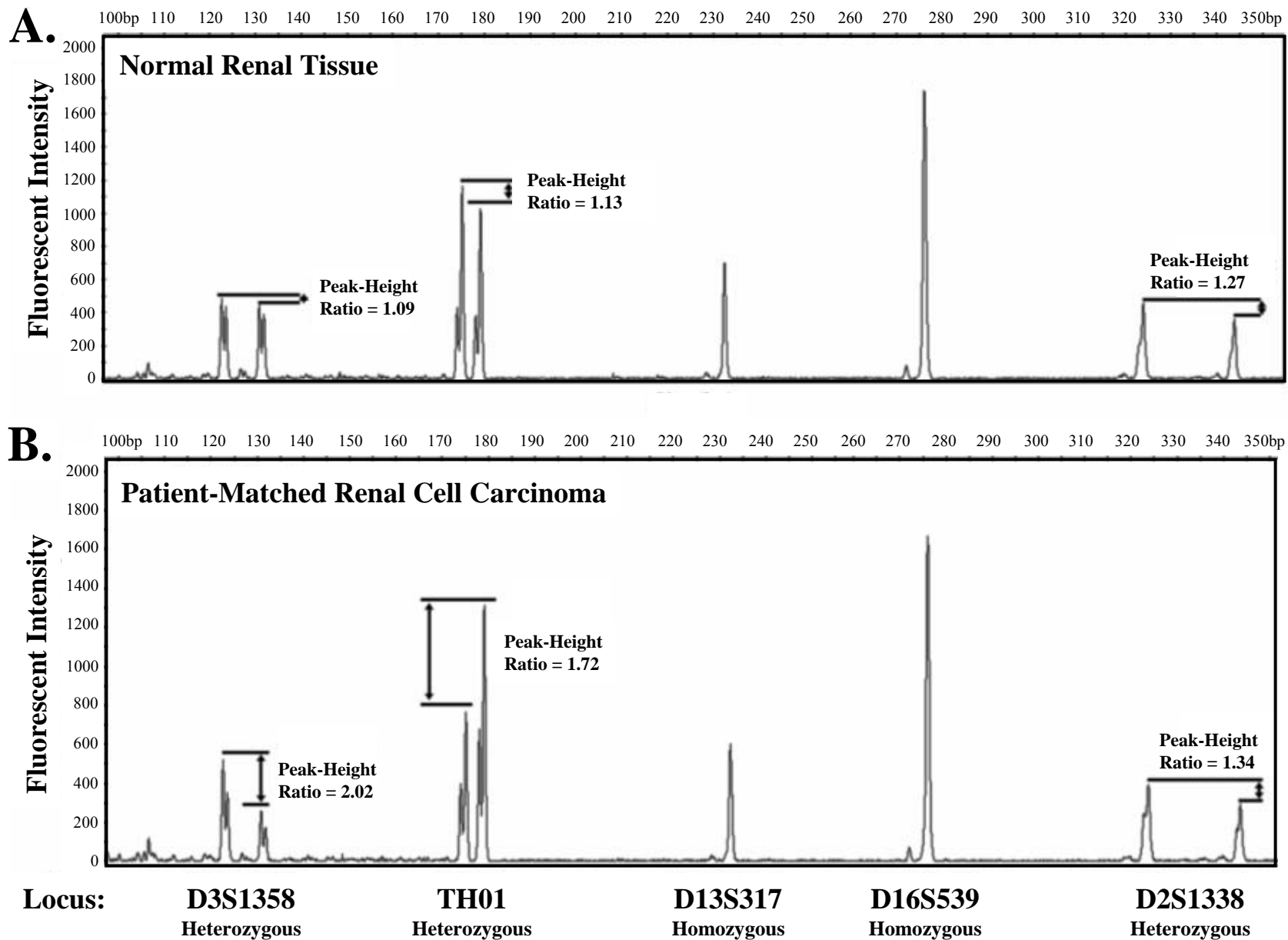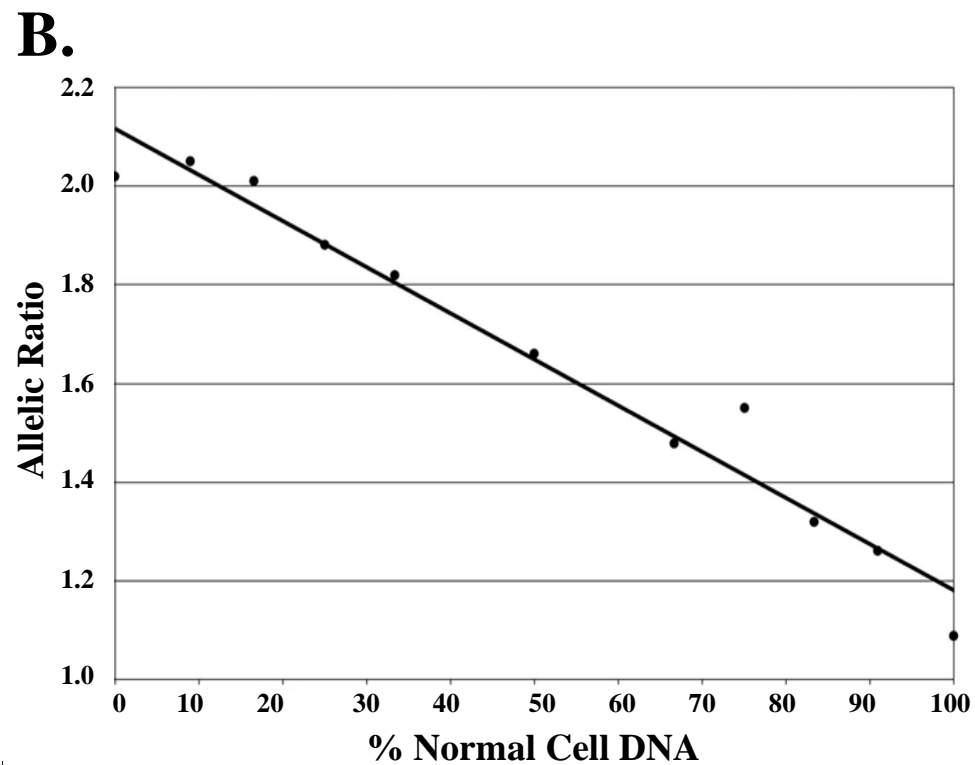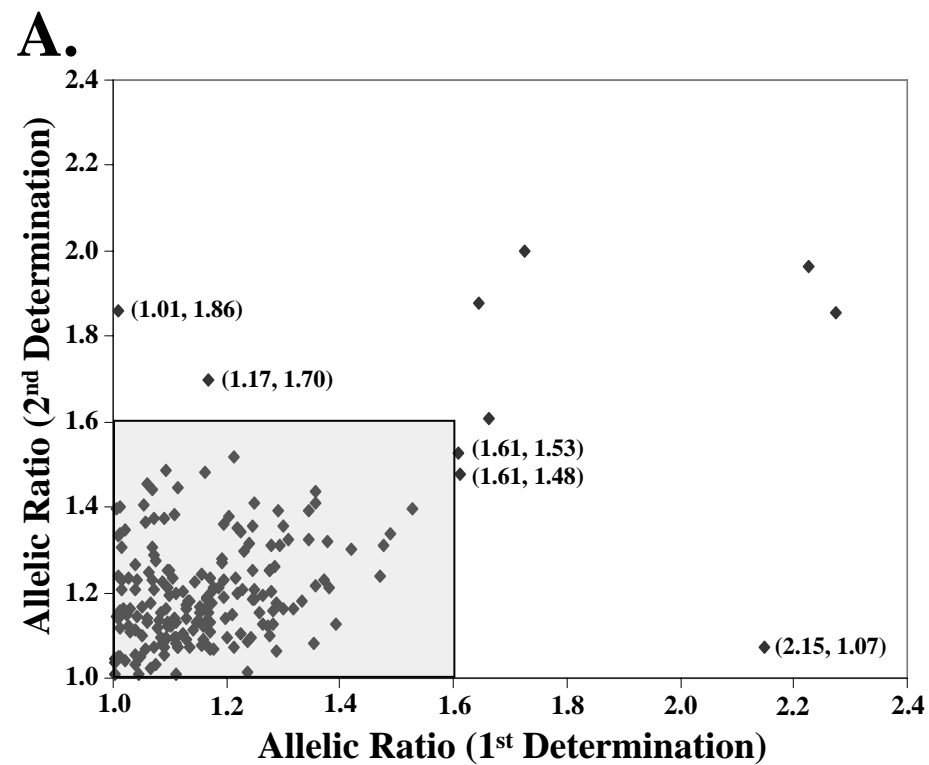
Figure Legends

Figure 1. Electropherograms of VIC-labeled amplicons from a matched normal and renal carcinoma sample. PCR was performed and the resulting amplicons resolved as described in Materials and Methods. Only VIC-labeled amplicons are shown. In this particular sample, the D3S1358, THO1 and D2S1338 loci are heterozygous and D13S317 and D16S539 loci are homozygous. Fluorescent intensity is shown on the y-axis and amplicon size, in base pairs, is shown on the x-axis. The ratios of the fluorescent intensities of each allelic pair of heterozygous loci are shown. Loci with allelic ratios of >1.60 are defined as sites of allelic imbalance for matched normal (A) or tumor (B) tissue.

Figure 2. Reproducibility and effect of admixtures of matched normal and renal carcinoma DNA on allelic peak height ratios. (A) Allelic peak height ratios were determined for 198 heterozygous loci in16 normal buccal samples. The plot represents the first determination (x-axis) and the second determination (y-axis). The region defined by the gray shaded box represents all the loci that were determined not to be a site of AI on both determinations. The labeled points (allelic peak height ratios for both determinations) represent the five loci that were not correctly identified upon repeating the experiment. (B) The specified admixtures were generated using DNA from a matched pair of normal renal tissue and renal cell carcinoma as shown in Figure 1. Data from the heterozygous D3S1358 locus are shown. The allelic ratios are 1.09 in the normal renal tissue and 2.02 in the renal carcinoma. The best-fit line was generated by linear regression and has a correlation coefficient (R^2) of 0.965.
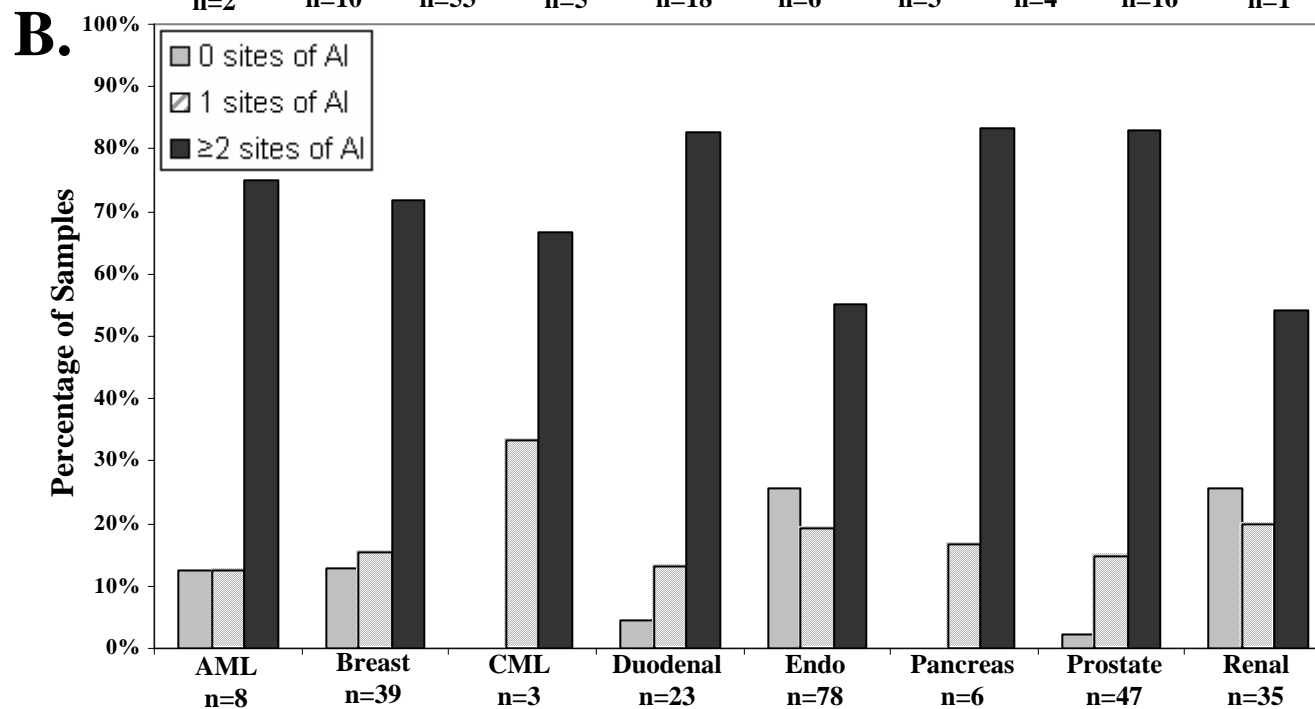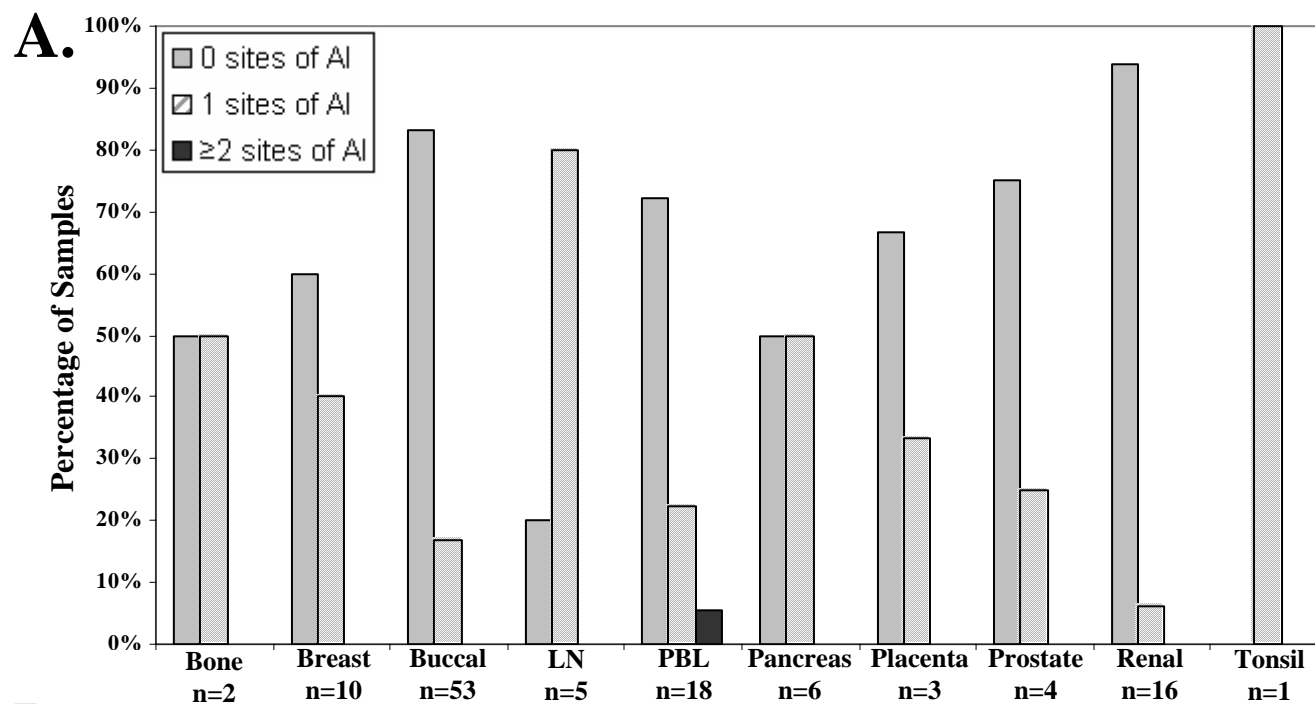
Figure 3. Frequency of allelic imbalance in normal and tumor tissues. The numbers of sites of allelic imbalance (i.e. 0, 1, ≥2) were determined in 118 samples of normal tissue (A) and in 239 samples of tumor tissue (B). The number of specimens in each tissue set (n) is indicated below the set designation. Abbreviations: Lymph Node: LN; Peripheral Blood Lymphocytes: PBL; Acute Myelogenous Leukemia: AML; Chronic Myelogenous Leukemia: CML; Endometrial: Endo. See Materials and Methods for additional details.

Figure 1

A.

Allelic Ratio (2nd Determination) vs Allelic Ratio (1st Determination)

(1.01, 1.86)
(1.17, 1.70)
(1.61, 1.53)
(1.61, 1.48)
(2.15, 1.07)

B.

Allelic Ratio vs % Normal Cell DNA

Figure 2

Figure 3

Appendix C

Telomere DNA content and allelic imbalance demonstrate field cancerization in histologically normal tissue adjacent to breast tumors

Christopher M. Heaphy[1], Marco Bisoffi[1,2], Colleen A. Fordyce[1], Christina M. Haaland[1], William C. Hines[1], Nancy E. Joste[2,3] and Jeffrey K. Griffith[1,2]*

[1]*Department of Biochemistry and Molecular Biology, University of New Mexico School of Medicine, Albuquerque, NM, USA*
[2]*Cancer Research and Treatment Center, University of New Mexico School of Medicine, Albuquerque, NM, USA*
[3]*Department of Pathology, University of New Mexico School of Medicine, Albuquerque, NM, USA*

Cancer arises from an accumulation of mutations that promote the selection of cells with progressively malignant phenotypes. Previous studies have shown that genomic instability, a hallmark of cancer cells, is a driving force in this process. In the present study, two markers of genomic instability, telomere DNA content and allelic imbalance, were examined in two independent cohorts of mammary carcinomas. Altered telomeres and unbalanced allelic loci were present in both tumors and surrounding histologically normal tissues at distances at least 1 cm from the visible tumor margins. Although the extent of these genetic changes decreases as a function of the distance from the visible tumor margin, unbalanced loci are conserved between the surrounding tissues and the tumors, implying cellular clonal evolution. Our results are in agreement with the concepts of ''field cancerization'' and ''cancer field effect,'' concepts that were previously introduced to describe areas within tissues consisting of histologically normal, yet genetically aberrant, cells that represent fertile grounds for tumorigenesis. The finding that genomic instability occurs in fields of histologically normal tissues surrounding the tumor is of clinical importance, as it has implications for the definition of appropriate tumor margins and the assessment of recurrence risk factors in the context of breast-sparing surgery.
© 2006 Wiley-Liss, Inc.

Genomic instability is an important factor in the progression of human cancers.[1–4] One mechanism that underlies genomic instability is loss of telomere function.[5–7] Telomeres are nucleoprotein complexes located at the ends of eukaryotic chromosomes. Telomeres in human somatic cells are composed of 1,000 to 2,000 tandemly repeated copies of the hexanucleotide DNA sequence, TTAGGG.[8] Numerous telomere binding proteins are associated with these repeat regions and are important for telomere maintenance.[9,10] Telomeres stabilize chromosome ends and prevent them from being recognized by the cell as DNA double-strand breaks, thereby preventing degradation and recombination.[11] However, telomeres can be critically shortened, and thereby become dysfunctional, by several mechanisms, including incomplete replication of the lagging strand during DNA synthesis,[12] loss or alterations of telomere-binding proteins involved in telomere maintenance,[13] and oxidative stress leading to DNA damage.[14] Alternatively, telomere loss may be compensated for by recombination[15,16] or, as seen in the majority of human cancers, by the enzyme telomerase.[17,18]

Telomeres in tumors are frequently shorter than in the matched adjacent normal tissues, presumably reflecting their extensive replicative histories.[19–21] The cause-and-effect relation between dysfunctional telomeres and genomic instability implies that shortened telomeres are also associated with altered gene expression. The latter is a primary source of phenotypic variability, which in turn drives the development of cell clones displaying progressively malignant traits, such as the potential for invasion and metastasis.[22] In agreement with this sequence of events, we and others have shown that telomere length, or its surrogate, telomere DNA content (TC), predicts the course of disease in several different malignancies, including leukemias,[23] non-small cell lung cancers,[24] neuroblastomas,[25] prostatic adenocarcinomas,[26–28] and breast carcinomas.[29,30]

Recently, Meeker and colleagues observed that telomere length abnormalities are early and frequent events in the malignant transformation of several types of cancer, including breast.[27,31,32] In addition, telomere attrition and other measures of genomic instability, such as allelic imbalance (AI) and loss of heterozygosity, demonstrate that genomic instability occurs within atypical breast hyperplasias,[33–35] histologically normal tissue proximal to breast tumors,[36–42] and, in some instances, breast tissue from women with benign breast disease.[43] Loss of heterozygosity and AI have also been found in the stromal compartment of cancer-associated breast tissues.[41,44] In addition, our own recent results identified fields of telomerase-positive cells within histologically normal tissues adjacent to breast tumors that could represent areas of premalignant cell populations.[45] Similarly, we have recently reported on the occurrence of telomere attrition in histologically normal prostatic tissue proximal to prostate adenocarcinomas.[28] These data imply that there is a reservoir of genetically unstable cell clones within histologically normal breast and prostate tissues that may represent fertile ground for tumor development. The origin and extent of this reservoir are presently undefined. However, the existence of fields of genetically altered cells, appearing histologically normal and disease-free, is consistent with the hypothesis that genomic instability arises early in breast tumorigenesis.

The primary goal of the present study was to define the extent and spatial distribution of genomic instability in histologically normal tissues surrounding breast tumors. A secondary goal was to investigate the relationship between genetic alterations in tumors and matched tumor-adjacent histologically normal (TA-HN) tissues. Towards these ends, two independent, yet conceptually linked markers of genomic instability, TC and AI, were investigated in two independent cohorts of breast tumors and their matched TA-HN tissues. One cohort represented a controlled study with tumors and matched TA-HN tissues excised at sites 1 and 5 cm from the tumor margins. The second cohort consisted of archival tumor specimens and matched TA-HN tissues excised at unknown distances from the tumor margin. Our results show that breast tumors reflect the properties of the matched TA-HN breast tissues, including the conservation of unbalanced alleles. Furthermore, our results support the hypothesis that fields of histologically normal, but genetically unstable cells provide a fertile ground for tumorigenic events in breast tissues.

Materials and methods

Breast tissue samples

Four independent cohorts of human breast tissues were used in this study. The characteristics of each of these cohorts are sum-

TABLE I – CLINICAL CHARACTERISTICS OF TUMOR COHORTS

Cohort	N	Age at Dx[1]			Dx[1]			Size[2]		Node[3]		TNM Stage						
		Range	Median	Mean	IDC	LC	DCIS	S	L	N	P	n/av	I	IIA	IIB	IIIA	IIIB	IV
1	12	26–61	53	49	10	1	1	n/av		2	10	2	0	3	2	2	3	0
2	38	35–75	48	50	36	2	0	4	32	7	29	2	2	5	14	11	0	2
3	48	31–89	54	56	44	4	0	8	40	19	29	0	11	13	15	8	1	0
4 (Normal)	20	15–48	30	29	n/a	n/a	n/a	n/a		n/a		n/a						

TNM, Tumor-Nodes-Distant Metastasis; n/a, not applicable; n/av, not available.
[1]Dx, Diagnosis of invasive ductal carcinoma (IDC), lobular carcinoma (LC), ductal carcinoma in situ (DCIS).–[2]S = small ($\leq$2 cm), L = large (>2 cm).–[3]N = negative, P = positive.

marized in Table I. The first cohort consisted of 12 full mastectomy cases obtained consecutively from the University of New Mexico (UNM) Hospital Surgical Pathology Laboratory in 2003 and 2004. Approximately 500 mg of tissue was excised from the tumors and sites 1 and 5 cm from the visible tumor margins. After resection, the tissues were immediately frozen in liquid nitrogen. Sections (10–12 μm) were prepared and stained with hematoxylin and eosin by the Human Tissue Repository Service of the UNM Department of Pathology. The sections were examined microscopically to define their histological status. In addition, serial sections of the breast tumors were collected and stored at −70°C until used for isolation of genomic DNA.

The second cohort was provided by the New Mexico Tumor Registry (NMTR) and consisted of 38 archival, paraffin-embedded ductal or lobular carcinomas and matched, histologically normal breast tissues from women who had undergone radical mastectomies or lumpectomies between 1982 and 1993. The histologically normal breast tissues originated from different blocks than the tumor tissues and were obtained at the time of dissection from sites outside the visible tumor margins. Generally, the sections were selected to contain high epithelial cell fractions.

The third cohort was obtained from the University of New Mexico Solid Tumor Facility and consisted of 48 frozen archival invasive ductal or lobular carcinomas from women who had radical mastectomies or lumpectomies between 1982 and 1993. Unlike cohorts 1 and 2, matched, histologically normal breast tissues were not available for the tumors in cohort 3.

The fourth cohort was obtained from the National Cancer Institute Cooperative Human Tissue Network (Nashville, TN) and contained 20 normal, disease-free breast tissue samples from women undergoing reduction mammoplasty (NBRST-RM). In addition, peripheral blood lymphocytes (PBLs) were obtained from 59 women previously diagnosed with breast cancer. The women ranged in age from 25 to 74 years, with a mean of 53 years. All tissues used in this study were anonymous, and experiments were performed in accordance with all federal guidelines as approved by the University of New Mexico Health Science Center Human Research Review Committee.

TC assay

Telomere length measurements can be affected by both extraneous factors, such as tissue specimens' age and means of preservation and storage, and inherent properties, such as patients' ages and health status, and the organ sites from which the tissue specimens were collected. To minimize the confounding effects of extraneous factors, we previously described a slot blot method for titrating the TC in fresh, frozen or paraffin-embedded tissues up to 20 years old.[46,47] TC measured by this method is directly proportional to telomere length measured by Southern blot.[47] However, in contrast to Southern blotting, the TC assay can be performed with as little as 5 ng of genomic DNA,[46] and is insensitive to fragmentation of DNA to less than 1 kb in length.[47] Thus, there is excellent agreement between TC measured in paired tissues stored either frozen, or formalin-fixed in paraffin at room temperature.[28,30] Therefore, TC is a sensitive and convenient proxy for telomere length, particularly for applications where genomic DNA is fragmented or scant, such as in sections of archival, paraffin-

embedded tissues comprising the second cohort of breast tumors, which contains specimens that are over 20 years old.

TC was measured as described previously.[46] Briefly, DNA was isolated from frozen or paraffin-embedded tissues and blood samples, using Qiagen DNeasy Tissue kits (Qiagen, Valencia, CA) and the manufacturer's protocols. DNA was denatured at 56°C in 0.05 M NaOH/1.5 M NaCl, neutralized in 0.5 M Tris/1.5 M NaCl, and applied and UV cross-linked to Tropilon-Plus blotting membranes (Applied Biosystems, Foster City, CA). A telomere-specific oligonucleotide, end-labeled with fluorescein, (5'-TTAGGG-3')$_4$-FAM (IDT, Coralville, IA), was hybridized to the genomic DNA, and the membranes were washed to remove nonhybridizing oligonucleotides. Hybridized oligonucleotides were detected by using an alkaline phosphatase-conjugated anti-fluorescein antibody that produces light when incubated with the CDP®-Star substrate (Applied Biosystems, Foster City, CA). Blots were exposed to Hyperfilm® for 2–10 min (Amersham Pharmacia Biotech, Buckinghamshire, UK) and digitized by scanning. The intensity of the telomere hybridization signal was measured from the digitized images, using Nucleotech Gel Expert Software 4.0 (Nucleotech, San Mateo, CA). TC is expressed as a percentage of the average chemiluminescent signal of three replicate tumor DNAs compared to the same amount of a placental DNA standard (typically 20 ng). In addition to placental DNA, DNA purified from HeLa cells, which has approximately 30% of placental TC was frequently included to confirm the reproducibility of the assay.

AI assay

DNA (approximately 1 ng) was amplified using the AmpFlSTR Identifiler PCR Amplification Kit (Applied Biosystems, Foster City, CA), using the manufacturer's protocol. Each multiplex PCR reaction amplifies 16 short tandem repeat (STR) microsatellite loci from independent locations in the genome (Amelogenin, CSF1PO, D2S1338, D3S1358, D5S818, D7S820, D8S1179, D13S317, D16S539, D18S51, D19S433, D21S11, FGA, TH01, TPOX and vWA). Each of the PCR primers is labeled with one of four fluorescent dyes (6-FAM, PET, VIC and NED), each with a unique emission profile, allowing the simultaneous resolution of 16 amplicons of similar size. PCR products were resolved by capillary gel electrophoresis and detected using an ABI Prism 377 DNA Sequencer (Perkin Elmer, Foster City, CA). The height of each fluorescence peak in the electropherograms was quantitated using the ABI Prism GeneScan and Genotype Analysis software (Applied Biosystems, Foster City, CA) and a ratio of the peak heights of each pair of heterozygous allelic amplicons was calculated. By convention, the allele with the greater fluorescence intensity was designated the numerator. Thus, the ratio was always $\geq$1.0, with 1.0 representing the theoretical ratio for normal alleles.

Statistical analysis

Statistical analyses were performed using the JMP® statistical package (SAS Institute, Cary, NC), choosing a significance level of 0.01. The nonparametric two-sided Wilcoxon/Kruskal–Wallis log rank test was used to determine the comparative distribution of TC and AI in the breast tumor and TA-HN tissue specimens, as well as associations between TC and AI in the paraffin-embedded breast tumor samples of cohort 2.
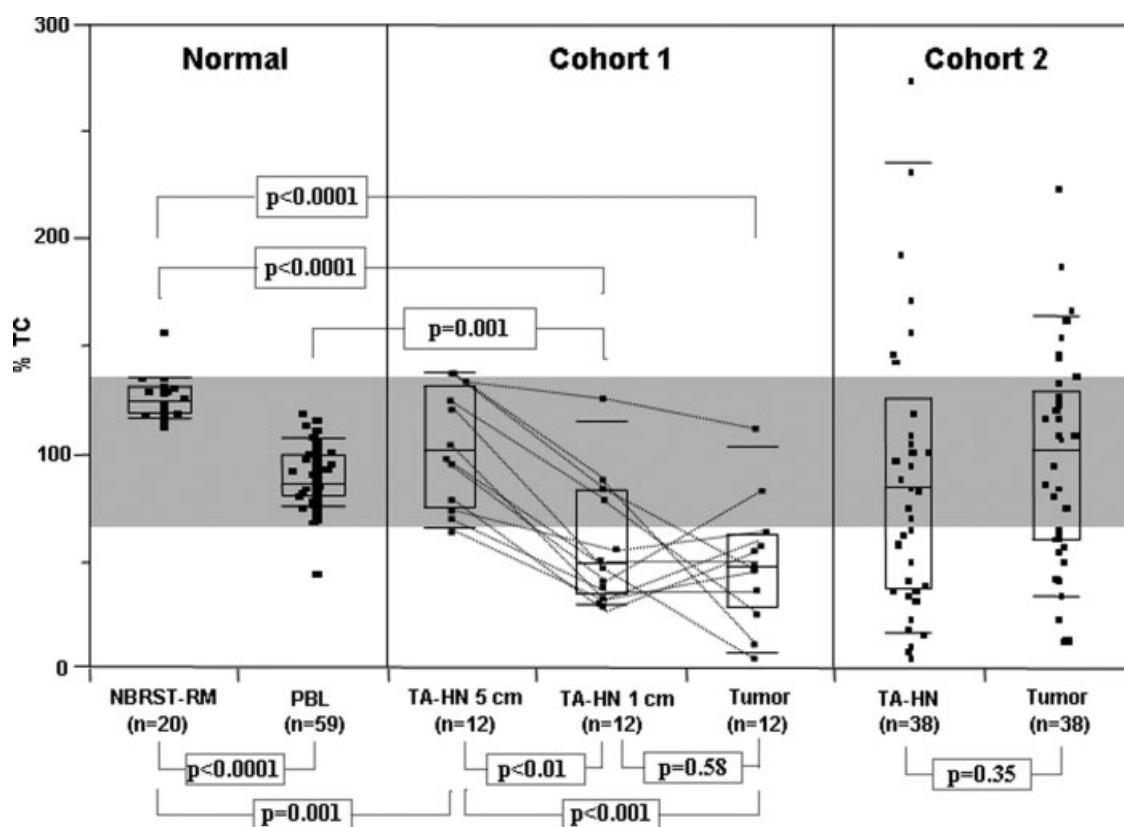
FIGURE 1 – Distribution of telomere DNA content (TC) in disease-free normal breast tissues from reduction mammoplasties (NBRST-RM), in peripheral blood lymphocytes (PBL), and in the breast tumor cohorts 1 and 2, including their tumor-adjacent histologically normal (TA-HN) tissues. TA-HN was excised at 1 and 5 cm from the tumor margin in cohort 1, and at unknown distances from the tumor margin in cohort 2. The number of tissues analyzed is indicated (*n*). TC is expressed as percentage of TC in placental control. The boxes represent group median (line across middle) and quartiles (25th and 75th percentiles) at its ends. Lines below and above boxes indicate 10th and 90th percentiles, respectively. In cohort 1, TC values of the individual matched samples are connected by thin lines. The gray shaded area indicates 95% of TC measurement for all normal specimens (NBRST-RM and PBLs). The *p*-values indicate comparisons between different tissue cohorts calculated by the two-sided Wilcoxon Kruskal/Wallis rank sums test. Additional statistical comparisons are mentioned in the text. *Note:* (i) Although the data points are horizontally shifted, some are still overlapping, and therefore not visible; (ii) due to the scale of the figure, two data points at values of 404% and 480% in the TA-HN set of cohort 2 are not shown.

Results

TC in normal breast tissues

To define the normal range of TC in disease-free breast tissues, the TC, a proxy for telomere length,[46,47] was measured in normal breast tissues obtained from 20 women (mean age 29) undergoing reduction mammoplasty (NBRST-RM). TC ranged from 114% to 158%, with a mean of 127% and a median of 126%, of TC in the placental DNA standard (Fig. 1). The interquartile variation (IQR), a statistical measure of the dispersion of the data, was only 12%, indicating little variation in telomere length in normal breast tissue. For comparison, TC was also measured in PBLs from 59 women (mean age 53) with a previous diagnosis of breast cancer. TC in PBLs ranged from 46% to 120%, with a mean of 90%, a median of 87% and an IQR of 19%, of the standard. The mean TC in normal breast was significantly higher than mean TC in PBLs ($p >$ 0.0001). However, greater than 95% of all normal specimens (NBRST-RM and PBLs) had TC values within 70–137% of the standard. This range is interpreted to include the effects of all extraneous and inherent factors on observed TC in normal tissue, including age, tissue site, sample source and experimental variation.

Histology of cancerous and adjacent histologically normal breast tissues

The histologies of the tissues comprising two representative cases from the two independent cohorts of breast tumor tissues and matched tumor adjacent histologically normal (TA-HN) tis-

sues are shown in Figure 2. The first cohort was composed of 12 sets of breast tumor tissues and TA-HN tissues excised 1 cm (TA-HN-1) and 5 cm (TA-HN-5) from the tumor margins. Frozen sections were stained with hematoxylin and eosin and examined microscopically. Sections of the tumors contained variable amounts of infiltrating carcinoma and ductal carcinoma *in situ* (Fig. 2*A* and 2*D*). In contrast, both TA-HN-1 and TA-HN-5 tissues had normal architecture, lobular units, ducts, and adipose tissue (Fig. 2*B*, 2*C* and 2*E*, 2*F*, respectively). Unlike the first cohort, which was composed of snap frozen tissues derived from contemporary mastectomies, the second was composed of paraffin-embedded archival tissues derived from women who had radical mastectomies or lumpectomies between 1982 and 1993. Fig. 2 shows two representative pairs of hematoxylin and eosin stained tumor (Fig. 2*G* and 2*I*) and TA-HN tissues (Fig. 2*H* and 2*J*). Infiltrating carcinoma can be seen in the tumors, while the TA-HN tissues show normal lobular architecture. Although tumor and TA-HN tissues comprising the second cohort came from different paraffin blocks, and the TA-HN tissues were obtained from sites outside the visible tumor margins, the exact distances between the sites of the TA-HN tissues and the tumors' margins are not known.

TC in tumor and adjacent histologically normal breast tissues

The spatial distribution of TC was examined in the 12 groups of breast tissues comprising the first cohort and compared with TC in the normal, disease-free breast tissues from radical mastectomy (Fig. 1). The mean TC values in the TA-HN-5 and TA-HN-1 tissues
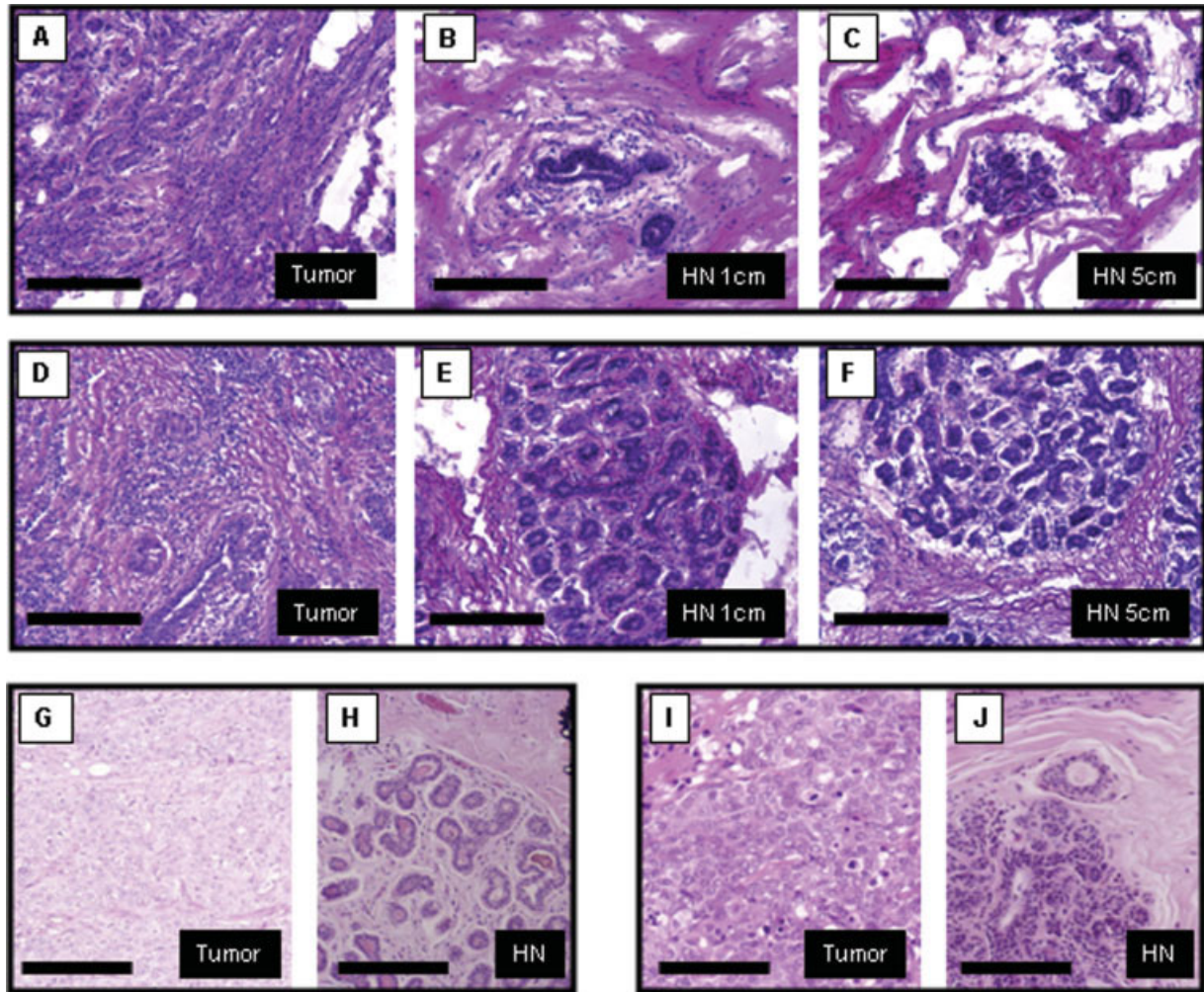
FIGURE 2 – Hematoxylin and eosin staining of human breast tissue sample sections. Two representative cases from the first (*A–F*) and second (*G–J*) cohorts are shown. Abnormal architecture with fields of infiltrating ductal carcinoma and ductal carcinoma *in situ* are seen in the tumor sections (A, D, G and I). Normal lobular and ductal architecture and adipose tissue are seen in the tumor-adjacent tissues at the indicated distance from the visible tumor margin (first cohort: B, C and E, F), or at unknown distances (second cohort: H and J). HN, histologically normal tissue; bars represent 200 μm.

were 101% and 66% of TC in the normal placental DNA standard, respectively. The mean TC value in tumors was 59%. Although the mean TC in TA-HN-5 tissues was significantly less than in NBRST-RM tissues ($p = 0.001$), it was not significantly different than the mean TC in PBLs from women of similar age ($p = 0.16$). Moreover, TC values in each of the TA-HN-5 tissues were within the range that defined >95% of all normal tissues. Since telomere length decreases with age,[48,49] it is likely that the difference between TC in the normal and TA-HN-5 tissues is due to the different ages of the two groups of women (27 *vs*. 49 years).

In contrast, mean TC in TA-HN-1 tissues was significantly less than TC in NBRST-RM tissues ($p < 0.0001$) and PBLs ($p = 0.001$), and TA-HN-5 tissues ($p < 0.01$). Mean TC in tumors also was significantly less than those in NBRST-RM tissues ($p < 0.0001$), PBLs ($p < 0.0001$) and TA-HN-5 tissues ($p < 0.001$). However, mean TC in tumor and TA-HN-1 tissues was indistinguishable ($p = 0.58$). Consistent with these findings, TC was, on average, 35% lower in each TA-HN-1 sample than in the paired TA-HN-5 sample, while the differences in TC between the TA-HN-1 and matched tumor specimens were varied, encompassing decrease, stabilization, and increase of TC with an average change of only 3% (lines in middle panel of Fig. 1). In total, TC values in 8 of 12 specimens of TA-HN-1 and 10 of 12 specimens of paired

tumor tissues were outside the range that defined >95% of all normal tissues (NBRST-RM and PBLs).

Similarly, TC distribution was examined in a second, independent cohort (Fig. 1). Although the distributions of TC values in the 38 matched pairs of TA-HN and tumor tissues were broader than those measured in the first cohort (IQR = 88% and 69%, respectively), 16 of 38 TA-HN and 14 of 38 tumor specimens, respectively, had TC values less than those found in NBRST-RM tissues and PBLs, and only 9 of 38 TA-HN and 7 of 38 tumor specimens had TC values exceeding those found in all normal tissues (NBRST-RM and PBLs). A similar TC distribution was observed in a third collection of 48 frozen breast tumors (Table II), and in a collection of archival tumor and matched TA-HN prostate tissues, each collected between 1982 and 1993.[28] As observed in the comparison between tumor and TA-HN-1 specimens in the first cohort, there was no difference in mean TC in tumors and TA-HN tissues ($p = 0.35$). However, there was greater heterogeneity in the samples of the second as compared to the first cohort. Nevertheless, data from both cohorts are consistent with the conclusion that significant telomere attrition, comparable to that observed in tumors, occurs in TA-HN breast tissue. Significant telomere attrition (to a level outside the range seen in >95% of all normal tissues) occurred (i) in almost 50% (24/50) of TA-HN-1 and TA-HN

specimens, (ii) at sites at least 1 cm from the tumors' margins, and (iii) since TC is measured in bulk tissue that has not been microdissected, in a substantial fraction of the cells in the samples.

AI in tumor and adjacent histologically normal breast tissues

To investigate the extent of genomic instability in cohorts 1 and 2, tumor and TA-HN tissues were screened for AI at 16 unlinked microsatellite loci. Unlike the TC assay, which utilizes a slot blot methodology to titrate the quantity of telomere DNA in a defined amount of genomic DNA, the AI is defined by the ratio of the peak heights of allelic amplicons after PCR. Thus, it is unlikely that inherent or extrinsic factors that affect measurement of TC would similarly affect the determination of AI. To establish a baseline for the incidence of AI in normal breast tissue, 201 heterozygous loci in the 20 specimens of NBRST-RM tissues were analyzed by this approach. The mean peak height ratio was determined to be 1.18 (SD = 0.166). On the basis of these values, a highly conservative, operational definition of AI was established as a ratio of peak heights ≥ 1.68, *i.e.*, the mean + 3.0 SD. This threshold excluded more than 99% of the allelic ratios observed in the NBRST-RM tissues, and established a baseline incidence of 0.1 unbalanced loci per specimen of normal breast tissue. As shown in Figure 3, a virtually identical value, 0.08 loci per specimen, was measured in the TA-HN-5 tissues. In contrast, the mean numbers of unbalanced loci in the TA-HN-1 and tumor tissues were 0.42 and 1.25 loci per specimen, respectively, approximately 5 and 15 times higher than the

incidence in the TA-HN-5 tissues. The baseline incidence of 0.1 unbalanced loci per specimen predicts that approximately 10% and 1% of normal tissues will have one and two unbalanced loci, respectively. Consistent with this prediction, 3 of 20 and 1 of 12 NBRST-RM and TA-HN-5 tissues, respectively, had one site of AI. Only one of more than 120 normal samples we have analyzed to date had 2 unbalanced loci, and none had more than 2 unbalanced loci. Accordingly, neither the NBRST-RM nor the TA-HN-5 specimens had more than one unbalanced locus. In contrast, one TA-HN-1, and 5 tumor tissues had 2 or more unbalanced loci. These data are consistent with the conclusion drawn from the TC analysis that both tumors and TA-HN-1 tissues are genetically distinct from TA-HN-5 tissue, and that both are genetically unstable.

This conclusion is further supported by results obtained with the second cohort. Microsatellite alleles were successfully amplified in 23 pairs of the 38 samples. As with the TC determinations, the distribution of the numbers of unbalanced loci was much broader in the second cohort than in the first. The mean numbers of unbalanced loci in the TA-HN tissues and matched tumors were 2.61 and 2.48 loci per specimen, respectively (Fig. 3). The mean numbers of unbalanced loci in TA-HN and tumor tissues were significantly greater than the numbers in either NBRST-RM or TA-HN-5 tissues ($p < 0.01$). The extent of AI in the tumors and their matched TA-HN tissues of the second cohort were indistinguishable ($p = 0.88$). Significantly, 74% (17/23) of TA-HN tissues and 70% (16/23) of matched tumors had 2 or more sites of AI, and 57% (13/23) and 40% (9/23), respectively, had 3 or more sites. Like the TC measurements, the independent measurement of AI, performed in two independent cohorts of paired breast tissues, indicates that at least 1 unbalanced locus is present (i) in more than 74% (26/35) of TA-HN-1 and TA-HN specimens, (ii) at sites at least 1 cm from the tumors' margins and (iii) since AI was measured in bulk tissue that was not microdissected, and the threshold for detecting AI requires that approximately 40% of the cells have lost the specific allele (see later), specific sites of AI are present in a substantial fraction of the cells.

Conservation of unbalanced alleles in tumor and adjacent breast tissues

To investigate the possibility that TA-HN and tumor tissues represented early and late stages, respectively, in the clonal evolution of the cancers, we measured the frequency of conservation of unbalanced loci in the 2 cohorts of paired tumor and TA-HN tissues. As shown in Figure 4, in the first cohort, 2 of the 6 (33%) sites of AI present in TA-HN tissues were conserved in the paired tumors (left panel). Likewise, in the second cohort, 21 of the 60

TABLE II – TC VALUES IN NORMAL, TUMOR AND TUMOR ADJACENT, HISTOLOGICALLY NORMAL (TA-HN) TISSUES[1]

	N	Median	Mean	Min	Max	IQR
Normal tissues						
NBRST-RM	20	126	127	114	158	12
PBL	59	87	90	46	120	19
Cohort 1						
TA-HN-5	12	100	101	70	128	44
TA-HN-1	12	59	66	43	119	38
Tumor	12	57	59	24	108	27
Cohort 2						
TA-HN	38	85	106	6	480	88
Tumor	38	102	98	14	224	69
Cohort 3						
Tumor	48	105	118	65	247	60

IQR, interquartile range; NBRST-RM, normal breast tissue from reduction mammoplasty; PBL, peripheral blood lymphocytes.
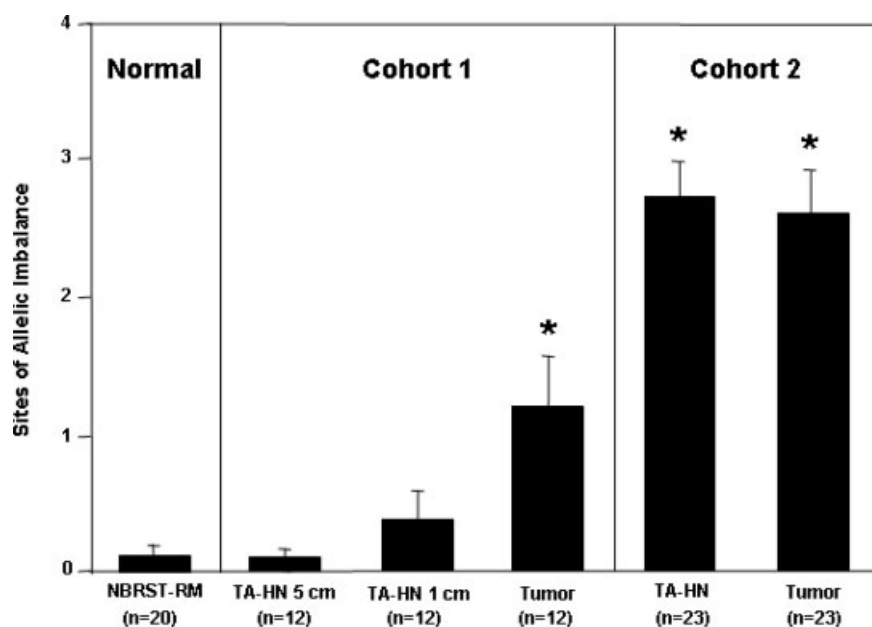[1]Data from Figure 1.

FIGURE 3 – Extent of allelic imbalance (AI) in disease-free normal breast tissues from reduction mammoplasties (NBRST-RM), and in the breast tumor cohorts 1 and 2, including their tumor-adjacent histologically normal (TA-HN) tissues. TA-HN was excised at 1 and 5 cm from tumor margin in cohort 1, and at unknown distances from the tumor margin in cohort 2. The number of tissues analyzed is indicated (*n*). The bars indicate the mean number of unbalanced loci ± standard errors. The stars indicate statistically significant differences ($p < 0.01$) from both NBRST-RM and TA-HN-5 (two-sided Wilcoxon Kruskal/Wallis rank sums test).
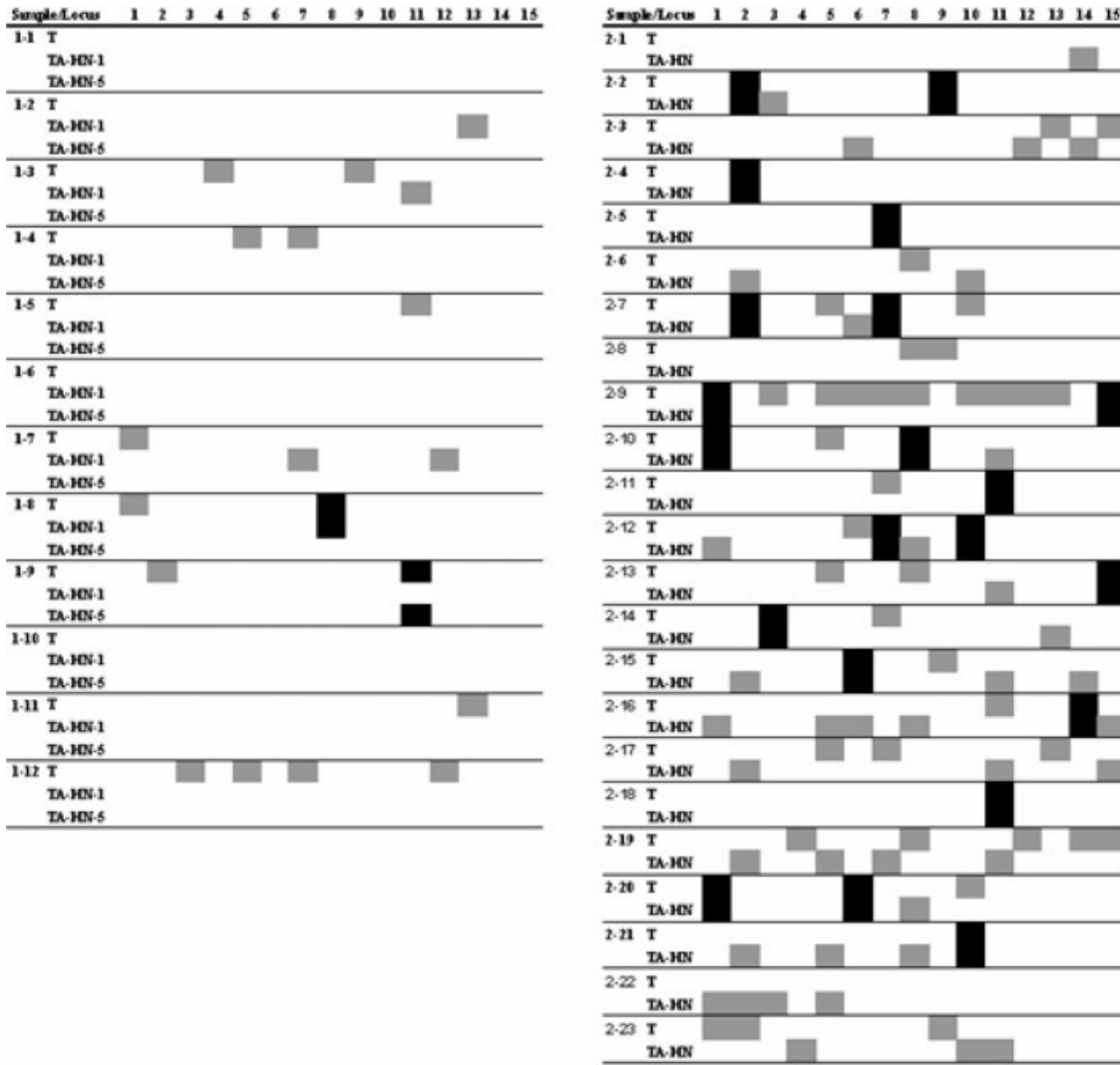
FIGURE 4 – Conservation of unbalanced alleles in matched tumor (T) and tumor-adjacent histologically normal (TA-HN) breast tissues of cohort 1 (left panel) and cohort 2 (right panel). Sites of allelic imbalances are indicated by gray boxes; sites of allelic imbalances conserved between tumor and TA-HN tissues are indicated by black boxes. The unlinked chromosomal loci are designated 1–15 and are as following (1) D8S1179, (2) D21S11, (3) D7S820, (4) CSF1PO, (5) D3S1358, (6) TH01, (7) D13S317, (8) D16S539, (9) D2S1338, (10) D19S433, (11) vWA, (12) TPOX, (13) D18S51, (14) D5S818, (15) FGA. *Note:* Homozygous amelogenin (all female samples) is not shown.

(35%) sites of AI present in TA-HN tissues were conserved in the paired tumors (right panel). The odds of this occurring by chance are estimated to be approximately 3×10^{-2} and 10^{-7} for the first and second cohorts, respectively.

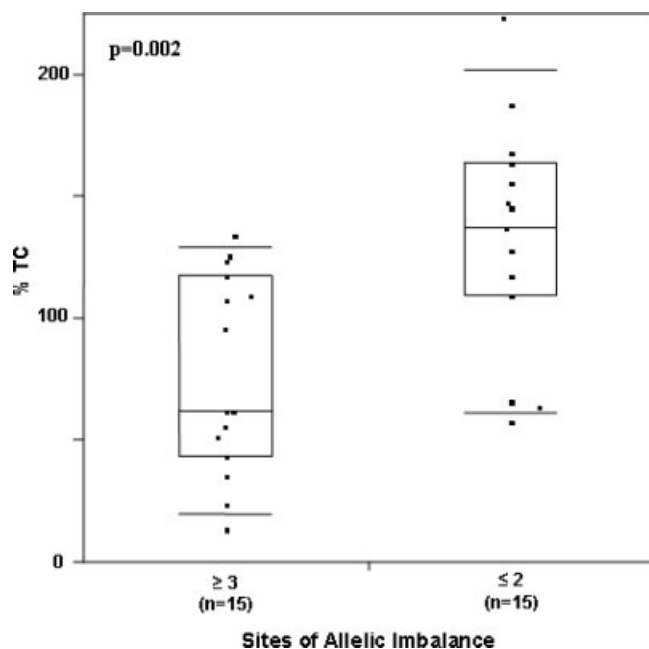*Association between TC and AI in breast tumor tissues*

Since telomere attrition is a source of genomic instability, and since we observed telomere attrition and increased AI in breast tumors, we determined the association between TC and AI (Fig. 5). For this analysis, microsatellite alleles were successfully amplified in 30 of the 38 breast tumor samples of cohort 2. Non-parametric 2-sided Wilcoxon/Kruskal–Wallis log rank analysis revealed a significant difference in TC in tumors with high (≥ 3 sites) as compared to low (≤ 2 sites) AI ($p = 0.002$).

Discussion

Although mechanistic insights into the molecular pathology of sporadic breast cancers are increasing, the question of how carcinogenesis is initiated in human breast tissues remains largely unanswered.[50–53] However, it is widely accepted that genomic instability is a prerequisite of virtually all tumors, including breast

cancers, and that this instability facilitates the accumulation of further genetic alterations that result in cancer progression through clonal expansion of cells with a proliferative advantage.[1–3,51–53]

Two independent, quantitative measures of genomic instability, TC and AI, were used in this study to demonstrate that genomic instability occurs in histologically normal breast tissues adjacent to the corresponding tumors. These studies show that shortened telomeres (to a level outside the range seen in >95% of all normal tissues) and unbalanced allelic loci are present (i) in 50–75% of TA-HN and TA-HN-1 specimens, (ii) at sites at least 1 cm from the tumor margins and (iii) in a substantial fraction of the cells comprising the TA-HN tissue. This finding parallels our previous studies on tumors of the prostate and their matched TA-HN tissues,[28] and is in agreement with the work of previous investigators who reported that genetic alterations, including telomere attrition and loss of heterozygosity, occur in histologically normal tissues adjacent to breast tumors.[34–38,41–44] In these previous studies, the sites of telomere attrition, loss of heterozygosity and AI were physically distant from one another and from the tumors, albeit in most cases at undefined distances from the corresponding tumor lesions.[24,42–44] In contrast, and to our knowledge, the findings in cohort 1 represent the first

FIGURE 5 – Association between telomere DNA content and allelic imbalance in 30 breast tumor samples of cohort 2. The samples were dichotomized according to the number of genomic sites affected by allelic imbalance, i.e. ≥ 3 or ≤ 2 sites. The number of tissues analyzed is indicated (*n*). TC is expressed as percentage of TC in placental control. The boxes represent group median (line across middle) and quartiles (25th and 75th percentiles) at its ends. Lines below and above boxes indicate 10th and 90th percentiles, respectively. The nonparametric two-sided Wilcoxon/Kruskal–Wallis log rank test was used to assess the statistical significance of the difference between the means.

study in breast cancers that analyzes genomic instability at defined distances (1 and 5 cm) from the visible tumor margins. Consequently, this study reveals that genomic instability in tumor adjacent, histologically normal breast tissues is a function of distance from the tumor lesion, showing decreasing extent of genomic instability with increasing distance from the tumor margin. One explanation for these findings is that breast tumor cells exert a transforming effect on surrounding cells, leading to genetic alterations in adjacent tissues, as has been proposed for prostate cancer cells.[54,55] However, we prefer the alternate hypothesis, that breast epithelial carcinogenesis occurs at higher frequency in fields of cells with elevated genomic instability. This is supported by our observation that the occurrence of two independent markers of genomic instability, telomere attrition and unbalanced allelic loci, are highest in the tumor lesions and decrease with increasing distance from the tumor. In addition, analysis of tumors reveals an association between TC and extent of AI. Thus, we argue that telomere attrition induces genomic instability in breast tissues, and while this may not necessarily be apparent in histologically normal precancerous tissue, it is strongly displayed in tumor lesions.

Although similar conclusions can be drawn from the TC and AI analyses in each of the two cohorts, the range of TC values and the number of unbalanced loci per specimen were both greater in the second cohort. In this context, it is important to emphasize that both TC and AI reflect the average TC and peak height ratios in the cells comprising the sample; they do not provide information about the variability of TC or AI *between* individual cells. Consequently, the ability to detect specific changes in TC or AI diminishes as the number and types of cells in the sample increases. On the basis of the DNA yields, we estimate that there were approximately 20 times more cells in the samples comprising the first cohort (median $\sim 10^6$ cells), than the second cohort (median $\sim 5 \times 10^4$ cells). This difference reflects the relative amounts of tissue available from the fresh surgical specimens comprising the first cohort versus the sec-

tions of paraffin-embedded tissue blocks comprising the second cohort. This consideration is particularly significant in the case of the AI assay. On the basis of theoretical considerations and mixing experiments (data not shown), we estimate that imbalance at a specific locus must occur in $\sim 40\%$ of the cells in the sample to generate an allelic ratio of 1.68, the threshold for significance used in these studies. Thus, sites of AI that are not prevalent in the cell population are not detected, even if there are many such individual sites. In this context, it is not surprising that specific sites of AI are detectable in breast tumors, which evolve clonally.[51] However, it is remarkable that AI is detected in TA-HN tissue, as it not only reflects underlying genomic instability, but also requires *clonal* expansion of genetically altered, premalignant cell clones within histologically normal breast tissues. This interpretation is further corroborated by the fact that more than a third of unbalanced alleles in adjacent, histologically normal tissues are conserved in the matched tumors. The latter has important practical implications, as it indicates that it is not necessary to micro-dissect tissues, for example using laser capture microscopy, to detect genomic instability, using the assays described in the present study. In fact, these assays allow the selective detection of changes in cell clones undergoing expansion because of proliferative advantages.

Taken together, our results are in agreement with the concept of ''field cancerization,'' introduced by Slaughter and colleagues in 1953,[56] and more recently reviewed by others.[57–59] These authors developed the term to explain the multifocal and seemingly independent areas of histologically precancerous alterations occurring in oral squamous cell carcinomas.[56] Organ systems in which field cancerization has been implied include lung, colon, cervix, bladder, skin and breast.[57] The concept of field cancerization has also been used to explain the occurrence of genetic and epigenetic mosaicism in cancer precursor tissues.[60] Based on our results, we propose to extend the concept of field cancerization to genetic alterations in otherwise histologically normal breast tissues, and our study is the first to include TC.

In head and neck squamous carcinoma, field cancerization has been shown for relatively large tissue areas, *i.e.* up to 7 cm in diameter.[61] It is thus not surprising that our data show extensive field cancerization in tissues 1 cm outside breast tumor margins. In the present study, TC was also different between disease-free NBRST-RM tissues and TA-HN tissues excised at 5 cm from the tumor margin. However, TC was similar in TA-HN-5 tissues and PBLs from women of similar age. Since telomere length decreases with age,[48,49] the observed difference in TC between NBRST-RM and TA-HN-5 tissues is likely due to the age discrepancy between the two cohorts of women (27 *vs.* 49 years).

The existence of fields of genomic instability that support tumorigenic events also has important clinical implications. First, such fields could give rise to clonal selection of precursor cells that ultimately lead to the development of cancer.[62] In this context, our recent studies have identified the presence of telomerase-positive cell populations within histologically normal tissues adjacent to breast tumors that could represent fields of premalignant cells.[45] Second, the presence of such fields, even after surgical resection of primary tumors, may represent an ongoing risk factor for cancer recurrence or formation of secondary lesions, which occurs in up to 22% of women undergoing breast conservation therapies for small invasive and noninvasive breast cancers.[58,63,64] For these reasons, our study has practical implications for the assessment of appropriate tumor margins for breast cancer surgical procedures, secondary treatment options and prognosis, possibly including the risk for the development of new primary tumors in the contra-lateral breast.[65–67] Thus, our study also suggests that evaluation of surgical margins should include molecular, in addition to histological, techniques, thus warranting further investigations.

Acknowledgements

References

1. Gollin SM. Chromosomal instability. Curr Opin Oncol 2004;16:25–31.
2. Charames GS, Bapat B. Genomic instability and cancer. Curr Mol Med 2003;3:589–96.
3. Nojima H. G1 and S-phase checkpoints, chromosome instability, and cancer. Methods Mol Biol 2004;280:3–49.
4. Lengauer C, Kinzler KW, Vogelstein B. Genetic instabilities in human cancers. Nature 1998;396:643–9.
5. Desmaze C, Soria JC, Freulet-Marriere MA, Mathieu N, Sabatier L. Telomere-driven genomic instability in cancer cells. Cancer Lett 2003;194:173–82.
6. Callen E, Surralles J. Telomere dysfunction in genome instability syndromes. Mutat Res 2004;567:85–104.
7. Hackett JA, Feldser DM, Greider CW. Telomere dysfunction increases mutation rate and genomic instability. Cell 2001;106:275–86.
8. Moyzis RK, Buckingham JM, Cram LS, Dani M, Deaven LL, Jones MD, Meyne J, Ratliff RL, Wu JR. A highly conserved repetitive DNA sequence, (TTAGGG)$_n$, present at the telomeres of human chromosomes. Proc Natl Acad Sci U S A. 1988;85:6622–6.
9. de Lange T. Protection of mammalian telomeres. Oncogene 2002;21:532–40.
10. Smogorzewska A, de Lange T. Regulation of telomerase by telomeric proteins. Ann Rev Biochem 2004;73:177–208.
11. Maser RS, DePinho RA. Telomeres and the DNA damage response: why the fox is guarding the henhouse. DNA Repair 2004;3:979–88.
12. Olovnikov AM. Principle of marginotomy in template synthesis of polynucleotides. Dokl Akad Nauk 1971;201:1496–9.
13. Smogorzewska A, van Steensel B, Bianchi A, Oelmann S, Schaefer MR, Schnapp G, de Lange T. Control of human telomere length by TRF1 and TRF2. Mol Cell Biol 2000;20:1659–68.
14. Bohr VA, Anson RM. DNA damage, mutation and fine structure DNA repair in aging. Mutat Res 1995;338:25–34.
15. Neumann AA, Reddel RR. Telomere maintenance and cancer—look, no telomerase. Nat Rev Cancer 2002;2:879–84.
16. Reddel RR. Alternative lengthening of telomeres, telomerase, and cancer. Cancer Lett 2003;194:155–62.
17. Greider CW, Blackburn EH. Identification of a specific telomere terminal transferase activity in tetrahymena extracts. Cell 1985;43:405–13.
18. Kim NW, Piatyszek MA, Prowse KR, Harley CB, West MD, Ho PL, Coviello GM, Wright WE, Weinrich SL, Shay JW. Specific association of human telomerase activity with immortal cells and cancer. Science 1994;266:2011–5.
19. Hastie N, Dempster M, Dunlop M, Thompson A, Green D, Alshire R. Telomere reduction in human colorectal carcinoma and with ageing. Nature 1990;346:866–8.
20. Furugori E, Hirayama R, Nakamura KI, Kammori M, Esaki Y, Takubo K. Telomere shortening in gastric carcinoma with aging despite telomerase activation. J Cancer Res Clin Oncol 2000;126:481–5.
21. Mehle C, Ljungberg B, Roos G. Telomere shortening in renal cell carcinoma. Cancer Res 1994;54:236–41.
22. Albertson DG, Collins C, McCormick F, Gray JW. Chromosome aberrations in solid tumors. Nat Genet 2003;34:369–76.
23. Ohyashiki JH, Sashida G, Tauchi T, Ohyashiki K. Telomeres and telomerase in hematologic neoplasia. Oncogene 2002;21:680–7.
24. Hirashima T, Komiya T, Nitta T, Takada Y, Kobayashi M, Masuda N, Matui K, Takada M, Kikui M, Yasumitu T, Ohno A, Nakagawa K, et al. Prognostic significance of telomeric repeat length alterations in pathological stage I–IIIA non-small cell lung cancer. Anticancer Res 2000;20:2181–7.
25. Hiyama E, Hiyama K, Yokoyama T, Ichikawa T, Matsuura Y. Length of telomeric repeats in neuroblastoma: correlation with prognosis and other biological characteristics. Jpn J Cancer Res 1992;83:159–64.
26. Donaldson L, Fordyce C, Gilliland F, Smith A, Feddersen R, Joste N, Moyzis R, Griffith J. Association between outcome and telomere DNA content in prostate cancer. J Urol 1999;162:1788–92.
27. Meeker AK, Hicks JL, Platz EA, March GE, Bennett CJ, Delannoy MJ, De Marzo AM. Telomere shortening is an early somatic DNA alteration in human prostate tumorigenesis. Cancer Res 2002;62:6405–9.
28. Fordyce CA, Heaphy CM, Joste NE, Smith AY, Hunt WC, Griffith JK. Association between cancer-free survival and telomere DNA content in prostate tumors. J Urol 2005;173:610–4.
29. Odagiri E, Kanada N, Jibiki K, Demura R, Aikawa E, Demura H. Reduction of telomeric length and c-erbB-2 gene amplification in human breast cancer, fibroadenoma, and gynecomastia. Relationship to histologic grade and clinical parameters. Cancer 1994;73:2978–84.
30. Griffith JK, Bryant JE, Fordyce CA, Gilliland FD, Joste NE, Moyzis RK. Reduced telomere DNA content is correlated with genomic instability and metastasis in invasive human breast carcinoma. Breast Cancer Res Treat 1999;54:59–64.
31. Meeker AK, Hicks JL, Iacobuzio-Donahue CA, Montgomery EA, Westra WH, Chan TY, Ronnett BM, De Marzo AM. Telomere length abnormalities occur early in the initiation of epithelial carcinogenesis. Clin Cancer Res 2004;10:3317–26.
32. Meeker AK, Argani P. Telomere shortening occurs early during breast tumorigenesis: a cause of chromosome destabilization underlying malignant transformation? J Mammary Gland Biol Neoplasia 2004;9:285–96.
33. O'Connell P, Pekkel V, Fuqua SA, Osborne CK, Clark GM, Allred DC. Analysis of loss of heterozygosity in 399 premalignant breast lesions at 15 genetic loci. J Natl Cancer Inst 1998;90:697–703.
34. Aubele MM, Cummings MC, Mattis AE, Zitzelsberger HF, Walch AK, Kremer M, Hofler H, Werner M. Accumulation of chromosomal imbalances from intraductal proliferative lesions to adjacent in situ and invasive ductal breast cancer. Diagn Mol Pathol 2000;9:14–9.
35. Farabegoli F, Champeme MH, Bieche I, Santini D, Ceccarelli C, Derenzini M, Lidereau R. Genetic pathways in the evolution of breast ductal carcinoma in situ. J Pathol 2002;196:280–6.
36. Deng G, Lu Y, Zlotnikov G, Thor AD, Smith HS. Loss of heterozygosity in normal tissue adjacent to breast carcinomas. Science 1996;274:2057–9.
37. Forsti A, Louhelainen J, Soderberg M, Wijkstrom H, Hemminki K. Loss of heterozygosity in tumour-adjacent normal tissue of breast and bladder cancer. Eur J Cancer 2001;37:1372–80.
38. Lakhani SR, Chaggar R, Davies S, Jones C, Collins N, Odel C, Stratton MR, O'Hare MJ. Genetic alterations in 'normal' luminal and myoepithelial cells of the breast. J Pathol 1999;189:496–503.
39. Kurose K, Hoshaw-Woodard S, Adeyinka A, Lemeshow S, Watson PH, Eng C. Genetic model of multi-step breast carcinogenesis involving the epithelium and stroma: clues to tumor-microenvironment interactions. Hum Mol Gen 2001;10:1907–13.
40. Moinfar F, Man YG, Arnould L, Bratthauer GL, Ratschek M, Tavassoli FA. Concurrent and independent genetic alterations in the stromal and epithelial cells of mammary carcinoma: implications for tumorigenesis. Cancer Res 2000;60:2562–6.
41. Larson PS, de las Morenas A, Bennett SR, Cupples LA, Rosenberg CL. Loss of heterozygosity or allele imbalance in histologically normal breast epithelium is distinct from loss of heterozygosity or allele imbalance in co-existing carcinomas. Am J Pathol 2002;161:283–90.
42. Meeker AK, Hicks JL, Gabrielson E, Strauss WM, De Marzo AM, Argani P. Telomere shortening occurs in subsets of normal breast epithelium as well as in situ and invasive carcinoma. Am J Pathol 2004;164:925–35.
43. Euhus DM, Cler L, Shivapurkar N, Milchgrub S, Peters GN, Leitch AM, Heda S, Gazdar AF. Loss of heterozygosity in benign breast epithelium in relation to breast cancer risk. J Natl Cancer Inst 2002;94:858–60.
44. Ellsworth DL, Ellsworth RE, Love B, Deyarmin B, Lubert SM, Mittal V, Shriver CD. Genomic patterns of allelic imbalance in disease-free tissue adjacent to primary breast carcinomas. Breast Cancer Res Treat 2004;88:131–9.
45. Hines WC, Fajardo AM, Joste NE, Bisoffi M, Griffith JK. Quantitative and spatial measurements of telomerase reverse transcriptase expression within normal and malignant human breast tissues. Mol Cancer Res 2005;3:503–9.
46. Fordyce CA, Heaphy CM, Griffith JK. Chemiluminescent measurement of telomere DNA content in biopsies. Biotechniques 2002;33:144–6, 8.
47. Bryant JE, Hutchings KG, Moyzis RK, Griffith JK. Measurement of telomeric DNA content in human tissues. Biotechniques 1997;23:476–8, 80, 82.
48. Baird DM, Kipling D. The extent and significance of telomere loss with age. Ann N Y Acad Sci 2004;1019:265–8.
49. Aviv A. Telomeres and human aging: facts and fibs. Sci Aging Knowl Environ 2004;51:43.
50. Mathieu N, Pirzio L, Freulet-Marriere MA, Desmaze C, Sabatier L. Telomeres and chromosomal instability. Cell Mol Life Sci 2004;61:641–56.
51. Simpson PT, Reis-Filho JS, Gale T, Lakhani SR. Molecular evolution of breast cancer. Mol J Pathol 2005;205:248–54.
52. Kenemans P, Verstraeten RA, Verheijen RH. Oncogenic pathways in hereditary and sporadic breast cancer. Maturitas 2004;49:34–43.
53. O'Connell P. Genetic and cytogenetic analyses of breast cancer yield different perspectives of a complex disease. Breast Cancer Res Treat 2003;78:347–57.
54. Pathak S, Nemeth MA, Multani AS, Thalmann GN, von Eschenbach AC, Chung LW. Can cancer cells transform normal host cells into malignant cells? Br J Cancer 1997;76:1134–8.

55. Ozen M, Multani AS, Kuniyasu H, Chung LW, von Eschenbach AC, Pathak S. Specific histologic and cytogenetic evidence for in vivo malignant transformation of murine host cells by three human prostate cancer cell lines. Oncol Res 1997;9:433–8.

56. Slaughter DP, Southwick HW, Smejkal W. Field cancerization in oral stratified squamous epithelium; clinical implications of multicentric origin. Cancer 1953;6:963–8.

57. Braakhuis BJ, Tabor MP, Kummer JA, Leemans CR, Brakenhoff RH. A genetic explanation of Slaughter's concept of field cancerization: evidence and clinical implications. Cancer Res 2003;63:1727–30.

58. Garcia SB, Park HS, Novelli M, Wright NA. Field cancerization, clonality, and epithelial stem cells: the spread of mutated clones in epithelial sheets. J Pathol 1999;187:61–81.

59. Hockel M, Dornhofer N. The hydra phenomenon of cancer: why tumors recur locally after microscopically complete resection. Cancer Res 2005;65:2997–3002.

60. Tycko B. Genetic and epigenetic mosaicism in cancer precursor tissues. Ann N Y Acad Sci 2003;983:43–54.

61. Braakhuis BJ, Leemans CR, Brakenhoff RH. Expanding fields of genetically altered cells in head and neck squamous carcinogenesis. Semin Cancer Biol 2005;15:113–20.

62. Ellsworth DL, Ellsworth RE, Liebman MN, Hooke JA, Shriver CD. Genomic instability in histologically normal breast tissues: implications for carcinogenesis. Lancet Oncol 2004;5:753–8.

63. Li Z, Moore DH, Meng ZH, Ljung BM, Gray JW, Dairkee SH. Increased risk of local recurrence is associated with allelic loss in normal lobules of breast cancer patients. Cancer Res 2002;62:1000–3.

64. Huston TL, Simmons RM. Locally recurrent breast cancer after conservation therapy. Am J Surg 2005;189:229–35.

65. Klimberg VS, Harms S, Korourian S. Assessing margin status. Surg Oncol 1999;8:77–84.

66. Singletary SE. Surgical margins in patients with early-stage breast cancer treated with breast conservation therapy. Am J Surg 2002;184:383–93.

67. Meric-Bernstam F. Breast conservation in breast cancer: surgical and adjuvant considerations. Curr Opin Obstet Gynecol 2004;16:31–6.